Received: 18 January 2022 | Accepted: 2 March 2022

DOI: 10.1002/ppj2.20042

The Plant Phenome Journal OPEN ACCESS

REVIEW AND INTERPRETATION

Segmentation of vegetation and microplots in aerial agriculture images: A survey

Sara Mardanisamani | **Mark Eramian**

Dep. of Computer Science, Univ. of Saskatchewan, 176 Thorvaldson, Saskatoon, SK, Canada

Correspondence
Sara Mardanisamani, Dep. of Computer Science, Univ. of Saskatchewan, 176 Thorvaldson, SK, Saskatchewan, S7N 5C9, Canada.
Email: sara.samani@usask.ca

Assigned to Associate Editor Michael Gore.

Abstract

Because of the increasing global population, changing climate, and consumer demands for safe, environmentally friendly, and high-quality food, plant breeders strive for higher yield cultivars by monitoring specific plant phenotypes. Developing new crop cultivars and monitoring through current methods is time-consuming, sometimes subjective, and based on subsampling of microplots. High-throughput phenotyping using unmanned aerial vehicle-acquired aerial orthomosaic images of breeding trials improves and simplifies this labor-intensive process. To perform per-microplot phenotype analysis from such imagery, it is necessary to identify and localize individual microplots in the orthomosaics. This paper reviews the key concepts of recent studies and possible future developments regarding vegetation segmentation and microplot segmentation. The studies are presented in two main categories: (a) general vegetation segmentation using vegetation-index-based thresholding, learning-based, and deep-learning-based methods; and (b) microplot segmentation based on machine learning and image processing methods. In this study, we performed a literature review to extract the algorithms that have been developed in vegetation and microplots segmentation studies. Based on our search criteria, we retrieved 92 relevant studies from five electronic databases. We investigated these selected studies carefully, summarized the methods, and provided some suggestions for future research.

Abbreviations: AP, affinity propagation; BPNN, back propagation neural network; CIVE, Color Index of Vegetation Extraction; CNN, convolutional neural network; COM1, Combined Indices 1; COM2, Combined Indices 2; CVIs, color vegetation indices; DCNN, deep convolutional neural network; EASA, environmentally adaptive segmentation algorithm; ECI, Elliptical Color Index; ExG, Excess Green; ExGR, Excess Green minus Excess Red; FLD, Fisher linear discriminant; GNDVI, Green normalized difference vegetation index; GRID, GReenfield Image Decoder; HI, Hue-intensity; HS, Hue-saturation; HSI, Hue-saturation-intensity; HSV, Hue-saturation-value; IPCA, index principal component analysis; MExG, Modified Excess Green; MFL, multifeature learning; MS-BPNN, mean-shift algorithm with back propagation neural network; MS-FLD, mean-shift Algorithm with Fisher linear discriminant; NDI, normalized difference index; NDVI, normalized difference vegetation index; NIR, near-infrared; PCA, principal component analysis; POIs, pixels of interest; RGB, red-green-blue; rgb, normalized red-green-blue; ROI, region of interest; SVM, support vector machine; UAV, unmanned aerial vehicle; VEG, vegetation index.

1 | INTRODUCTION

In the coming decades, those involved with food production will face challenges related to the increasing global population, the changing climate, and consumer demands for safe, environmentally friendly, and high-quality food. Farmers and plant breeders are looking for new, superior plant cultivars to meet these challenges. Developing new cultivars through current methods is time-consuming, subjective, based on manual assessment, and prone to error. Many cultivars of a species must be sown, and breeders must go from microplot to microplot, visually assigning scores based on qualitative and quantitative traits of plants and ranking the plants at multiple stages of development. Image-based phenotyping has the potential to decrease the error of this subjective process and provide faster monitoring of a large number of plants at the same time (Araus & Cairns, 2014; Chawade et al., 2019).

An unmanned aerial vehicle (UAV), an aircraft piloted by remote control, collects high-resolution aerial images from the entire field. The UAVs play a vital role in carefully monitoring the large area of farmland and considering slope and elevation factors (Pinguet, 2021). Crucially, the high-resolution UAV data can be used to allow professionals to apply fertilizer accurately, reduce wastage, assess the fertility of crops, plan irrigation systems, and troubleshoot them. For example, significant cost and environmental savings can be made by optimizing fertilizer treatment and applying only the right amount at the right time (Xu et al., 2021). In addition, UAVs can be helpful to follow natural disasters, such as a flood, to help farmers assess damage across areas that may not be readily accessible on foot (Adams & Friedland, 2011; Sishodia et al., 2020).

Studies have shown that drone imagery provides high-resolution data with a higher accuracy rate even in challenging weather conditions (Chang et al., 2020; Maresma et al., 2016). Furthermore, UAVs can make accurate crop health assessments throughout the year, whereas using traditional data collection methods could potentially delay projects for days in challenging weather conditions (Chang et al., 2020; Pinguet, 2021; Sishodia et al., 2020).

Image-based phenotyping uses image-processing and machine-learning methods to obtain quantitative measurements of plants' structural and functional properties. This technique monitors plant growth, health, and physical traits from aerial drone-acquired images to provide a faster and more accurate assessment of the area within a field (Araus & Cairns, 2014; Xu et al., 2019). To provide a complete view of all microplots in the field, aerial images are stitched together using software to generate an orthomosaic image. Subsequent analysis requires the precise locations and identities of each microplot in the orthomosaic image (Duan et al., 2017; Guo et al., 2018). Thus, a fundamental step of these phenotypic studies on field trials is detecting and localizing research microplots within the field. Microplots may or may not be planted in rectangular-shaped areas. Even if they are in a grid-like arrangement, the orthomosaic may be warped due to inaccuracies in geolocation information on the drone, which can cause slight spatial warping during the image stitching process used to generate the orthomosaic. Such spatial warping can make microplot localization more challenging because microplot boundaries that are expected to be perfectly straight are not. Figure 1 shows the red-green-blue (RGB) orthomosaic images from canola and the normalized difference vegetation index (NDVI) images from wheat (*Triticum aestivum* L.) breeding trial fields in early, mid-, and late seasons.

Hamuda et al. (2016) observed that natural illumination affects the performance of plant segmentation algorithms, and poor illumination conditions contribute to poor plant segmentation. Thus, an area of focus within our survey is the performance of image processing and machine learning techniques for plant/microplots segmentation under various field conditions, including illumination.

Figure 2 shows a canonical flowchart of a general scheme for vegetation segmentation and microplot segmentation. There are three general approaches to segment plants/microplots from the background/soil in the literature. The first approach uses color vegetation indices (CVIs) to create a feature map, followed by thresholding of the feature map to obtain segmented images (red, solid path in Figure 2). The second approach uses thresholded CVI feature maps as input to traditional machine-learning-based algorithms that produce segmentations from the input image, feature map, and/or thresholded feature map (green, dashed path in Figure 2). The final approach uses CVI feature maps as inputs for training deep-learning-based models to segment plants or microplots (blue, dotted path in Figure 2). After obtaining the segmented images using one of the three approaches, microplots are extracted and associated with their plot identifiers from the breeding trial. Finally, some postprocessing steps may be applied, and then phenotypic traits are extracted.

Core Ideas

- Algorithms that are commonly used for vegetation segmentation in the field are reviewed.
- The state-of-the-art algorithms in vegetation segmentation are presented.
- The state-of-the-art algorithms for microplot segmentation in the field are reviewed.
- Challenges created by lack of and gaps between plots in microplot segmentation in the field are analyzed.
- Recommendations are given on algorithms and direction of future research for vegetation and microplot segmentation.

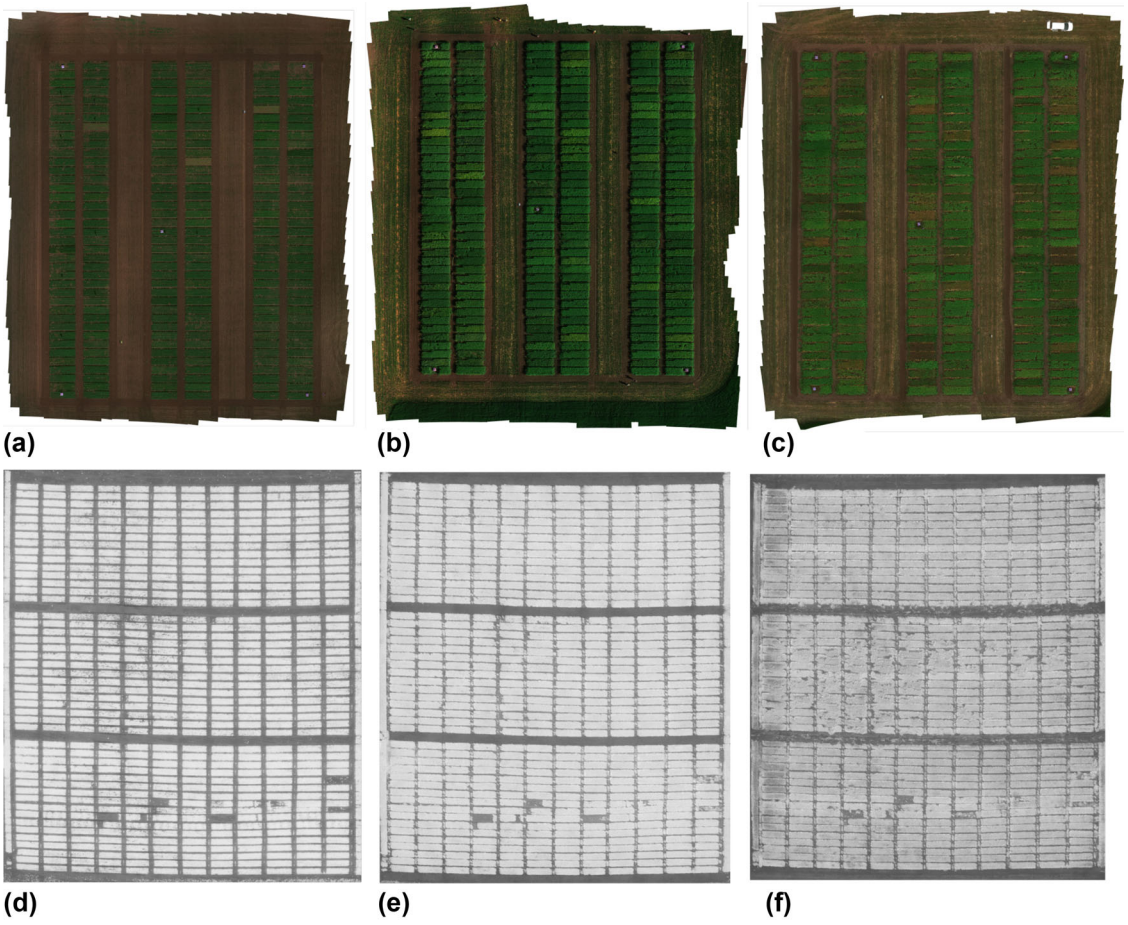

FIGURE 1 Image samples. Red-green-blue orthomosaic images on the canola dataset (a) in early season, (b) mid-season, (c) late-season images. Normalized difference vegetation index images on the wheat dataset (d) in early season, (e) mid-season, and (f) late-season images

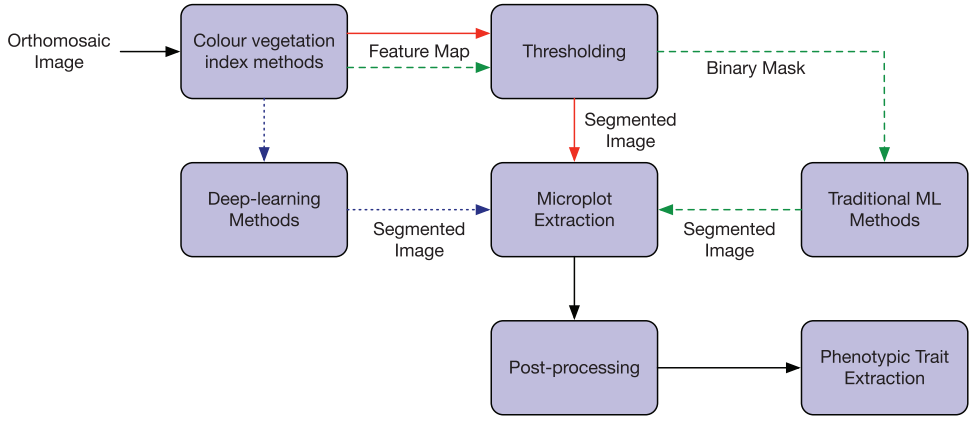

FIGURE 2 A canonical flowchart for microplot segmentation using color vegetation index thresholding methods (red, solid path), traditional machine learning methods (dashed green path) and deep learning methods (dotted blue path)

In the next sections, we review specific examples in the literature of each general approach in the canonical pipeline. The rest of the paper is structured as follows: Section 2 describes the literature search methodology. Section 3 reviews vegetation and plant segmentation methods in general. Section 4 reviews the segmentation of specifically microplots in aerial agriculture images. Section 5 presents an over-arching discussion of findings in the

literature, a discussion of future directions, and concludes this paper.

2 | METHODOLOGY

2.1 | Database search and research questions

There are several reviews of image processing and machine learning techniques for plant segmentation (Hamuda et al., 2016), weed detection (Wang et al., 2019), and weed/crop segmentation and identification (Kumar & Prema, 2013) or review papers that target deep learning in agriculture (Kamilaris & Prenafeta-Boldú, 2018). However, none of them reviewed microplot segmentation using UAV-acquired imagery. To our knowledge, our survey paper is the first review of microplot segmentation, which investigates extensive aspects, considerations, limitations, platforms, and applications in this field.

We defined a search methodology before conducting the literature review. First, we identified research questions to be answered by the review. Then, we selected databases in which to search. The databases used in this study are Science Direct, Springer Link, and Google Scholar. Next, we selected the search terms/keywords to be used to search the databases and a set of inclusion and exclusion criteria. Works found using the search terms/keywords were assessed and filtered using the exclusion and inclusion criteria. All the relevant data from the selected studies are extracted and summarized in response to the research questions.

We conducted our review with the goal of answering the following questions regarding vegetation segmentation in agricultural fields:

Q1: What algorithms are commonly used for vegetation segmentation in the field?

Q2: What algorithms are considered state-of-the-art in vegetation segmentation?

Q3: How can deep learning be used to segment vegetation in images?

To address these questions, we conducted searches utilizing Google Scholar (https://scholar.google.com), Springer Link (https://link.springer.com), and ScienceDirect (https://www.sciencedirect.com) using the following phrases: P1: Segmentation vegetation using image processing techniques; P2: Vegetation segmentation using learning-based methods; and P3: Aerial vegetation segmentation.

2.2 | Inclusion and exclusion criteria

Due to vast literature on vegetation segmentation, research papers had to meet the following inclusion and exclusion criteria.

2.2.1 | Inclusion criteria

1. Articles considering any of the following vegetation segmentation aspects: color-index based, threshold-based, learning-based, and deep-learning-based methods.
2. Articles where the main subject is any of: microplot localization and segmentation, or plant/vegetation segmentation.

2.2.2 | Exclusion criteria

1. Articles on disease spot segmentation or nutrient contents segmentation.
2. Articles that use CVI methods that have not been used in comparative studies.
3. Articles on crop row detection.
4. Articles exclusively on the subject of weed detection and segmentation.
5. Articles on studies that do not use image processing or machine learning methods
6. Articles published before 2000.
7. Articles not published in the English language.

2.3 | Summary of initial search results

Using phrase P1, we found a survey paper of image processing methods for plant segmentation (Hamuda et al., 2016). It was evident in this survey that vegetation segmentation algorithms can be categorized into four types: color index-based, threshold-based, learning-based, and deep-learning-based segmentation approaches. Based on these categories, we have explored papers that use different types of segmentation algorithms since the year 2000.

Using phrase P2, we searched the selected databases for methods in each category using search terms color index-based vegetation segmentation, threshold-based vegetation segmentation, learning-based vegetation segmentation, and deep-learning-based vegetation segmentation, respectively.

Using phrase P3, most of the papers found were related to vegetation segmentation in natural environments and urban areas. After considering papers found by the search, we found the state-of-the-art of microplot segmentation papers. As a result, we added two additional questions to be answered by this review:

Q4. What state-of-the-art algorithms work well in microplot segmentation in the field?

Q5. What are the future directions and research gaps?

To address these questions, we conducted searches utilizing Google Scholar, Frontiers website, and Plant Phenomic website (https://spj.sciencemag.org/journals/plantphenomics/) using phrase P4: P4: Automated segmentation of microplot

TABLE 1 Distribution of the selected papers based on the databases

Database	No. of initially retrieved papers	No. of papers after exclusion and inclusion criteria	Percentage of papers
Google Scholar	193	68	73.91%
Science Direct	38	13	14.13%
Springer Link	17	11	11.95%
Total	248	92	100%

TABLE 2 Summary of Selected Journals and Conferences

Scientific sources	Journals	Conferences	Preprint	Others	Total no. of papers
IEEE	6	5	–	–	11
Springer	3	6	–	–	9
Elsevier	30	–	–	–	30
Frontiers	3	–	–	–	3
MDPI	5	–	–	–	5
arXiv (Preprint)	–	–	1	–	1
Other journals	20	–	–	–	20
Other conferences	–	11	–	–	11
Thesis	–	–	–	2	2
Total	67	22	1	2	92

from orthomosaic images. Using phrase P4, we found about 25 papers on object detection/segmentation in agricultural images using the same inclusion/exclusion criteria and identified 13 of them as relevant. These papers are discussed in Section 4.

Searching the selected databases with the selected search terms yielded 248 papers, 92 of which met the inclusion and exclusion criteria, including 67 journal papers, 22 conference papers, three thesis, symposium, or preprint papers. Table 1 shows the distribution of these 92 over the databases in which they were found. Table 2 shows the distribution of the 92 selected papers by publisher. These 92 papers are discussed in Section 3.

3 | VEGETATION AND PLANT SEGMENTATION

Plant phenotyping and other agricultural applications, such as weed detection, mainly depend on using machine learning or image processing approaches to extract the relevant information to achieve the targeted goals of these applications. For most phenotyping applications, vegetation segmentation is the initial step to achieve the objective of each application (Hamuda et al., 2016; Burgos-Artizzu et al., 2011). Generally, this amounts to the classification of image pixels into crop/weed and soil/background classes. As presented in Figure 3, these methods typically

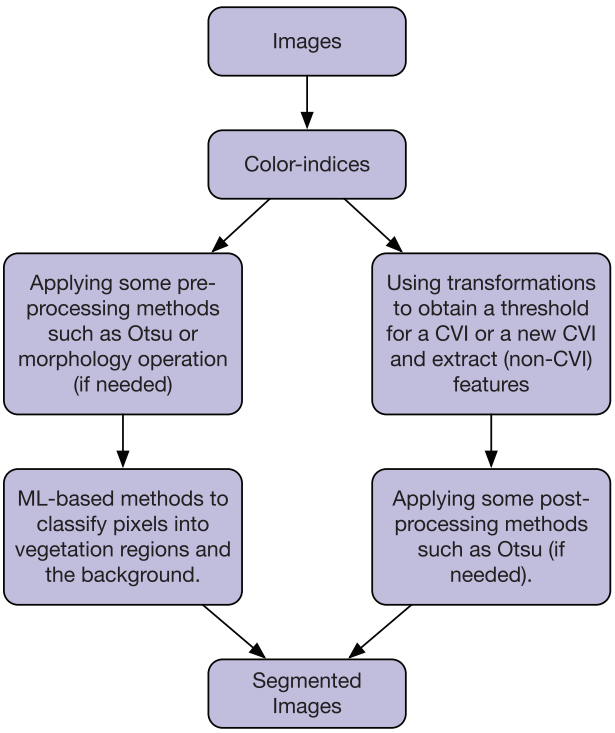

FIGURE 3 A summary flowchart of machine learning methods for vegetation/plant segmentation. This diagram adds detail on methodological variation for the traditional machine learning path (dashed green path) in Figure 2. CVI, color vegetation index.

take one of three general approaches that we now discuss in turn.

3.1 | Vegetation-index-based thresholding approaches

3.1.1 | Vegetation-index-based approaches

This section gives an overview of the recent development of vegetation segmentation using CVI methods. Most works use color indices to extract features that enable effective and efficient segmentation. We have selected 1 commonly used indices and compare and contrast their performance. A summary of the color indices used in the literature for vegetation segmentation is shown in Table 3.

From Table 3, it can be seen that most CVIs are mathematically defined in the RGB color space, and many can be expressed as a linear combination of R, G, and B channels:

$c_1 \times R + c_2 \times G + c_3 \times B + k$ where c_1, c_2, c_3, and k are real-valued coefficients. Different sets of coefficients have been determined to cope with specific segmentation situations, leading to the large number of CVIs that we find. However, none of these indices guarantee the best performance across different vegetation species or can be adapted to all vegetation segmentation scenarios (Wang et al., 2019; Lee et al., 2020). Hamuda et al. (2016) presented nine CVIs and summarized their advantages and disadvantages. Wang et al. (2019) categorized more than 20 CVIs into three groups:

1. CVIs derived either from RGB channels or normalized red-green-blue (rgb) channels (r, g, and b are the chromatic coordinates):

$$r = \frac{R^*}{R^* + G^* + B^*} \; g = \frac{G^*}{R^* + G^* + B^*} \; b = \frac{B^*}{R^* + G^* + B^*}$$

where R^*, G^*, and B^* are the normalized RGB values between 0 and 1 defined as:

$$R^* = \frac{R}{R_{\max}} \; G^* = \frac{G}{G_{\max}} \; B^* = \frac{B}{B_{\max}}$$

and R, G, and B are the actual pixel values from the images based on each RGB channel and $R_{\max}$, $G_{\max}$, and $B_{\max} = 255$ are the largest values of the RGB channels (Hamuda et al., 2016; Meyer & Neto, 2008).

1. CVIs generated by a combination of visible and invisible wavebands.
2. CVIs generated by other means. Usually these derived from R, G, and B channels that do not have the form of Equation (1) such as vegetation index (VEG), Combined Indices 1 (COM1), Combined Indices 2 (COM2), and Modified Excess Green (MExG) (Biswas et al., 2020; Hamuda et al., 2016; Hassanein et al., 2018), but some studies use r, g, and b normalized channels such as the indices Hue and Elliptical Color Index (ECI) (Golzarian & Frick, 2011; Lee et al., 2020; Yang et al., 2015). The normalized channels are more robust to variations in illumination (Cheng et al., 2001).

Table 4 summarizes recent studies of CVIs used on specific crops, the indices used in the studies, and the conclusion of which index resulted in the best performance on the study's task.

The most commonly used CVIs from Table 4 are Excess Green (ExG), Excess Green minus Excess Red (ExGR), Color Index of Vegetation Extraction (CIVE), Hue, COM1, and COM2. The ExG index, proposed by Woebbecke et al. (1995) distinguishes well between vegetation and bare soil; however, it does not perform well when illumination is too high or low. ExGR was developed by Meyer et al. (2004) and is defined as the difference between ExG and ExR = 1.3 × R – G. ExGR outperformed ExG for segmentation of vegetation from soil-residue background because ExR was used to eliminate the background where stems and branches (green-red material) may exist. The CIVE was proposed by Kataoka et al. (2003) for use with images of soybean and sugar beet fields. Hamuda et al. (2016), in their review paper, showed that CIVE outperformed ExG in green vegetation images without shadows and had good adaptability in the outdoor environment, but it does not perform well when illumination is weak or strong. Yang et al. (2015) used the Hue index to improve the robustness of the greenness identification for vegetation segmentation tasks in various illumination conditions. The proposed method worked well across a broad range of illumination conditions, is effective for images with complex backgrounds, and is robust to the variation of illumination within a field. Guijarro et al. (2011) selected four color indices (ExG, CIVE, ExGR, and VEG) and combined them to obtain the COM1 index to improve vegetation segmentation performance. They found that COM1 can solve the problem of oversegmentation (where background is deemed to be vegetation) or undersegmentation (where vegetation is deemed to be background). However, segmenting vegetation using COM1 increases the computational time and may segment shadows as part of the plant. Guerrero et al. (2012) also proposed the COM2 index, which is similar to COM1 but combines only ExG, CIVE, and VEG. The ExGR was excluded from COM1 because it was found to be the cause of shadows being classified plants in maize (Zea mays L.) crop images. The contribution of each index that comprises COM1 and COM2 is controlled by weights such that summation of the weights is 1. Hamuda et al. (2016) showed that COM2 was suitable for various outdoor environments caused by sunny or cloudy days; COM2 is less computationally

TABLE 3 Color-index based methods for vegetation segmentation

#	Color index	Description	Color space	Formulation	Reference
1	NDI	Normalized difference index	RGB	$NDI = 128 \times [(\frac{G-R}{G+R}) + 1]$	Woebbecke et al., 1993
2	ExG	Excess Green Index	rgb	$ExG = 2g - r - b$	(Woebbecke et al., 1995; Guerrero et al., 2012; Saha et al., 2016) (Torres-Sánchez et al., 2015; Barbosa et al., 2019)
3	ExGR	Excess Green minus Excess Red	RGB	$ExGR = ExG - ExR$	(Meyer et al., 2004; Meyer & Neto, 2008; Neto, 2004)
4	CIVE	Color Index of Vegetation Extraction	RGB	$CIVE = 0.441R - 0.811G + 0.385B + 18.78745$	(Guerrero et al., 2012; Kataoka et al., 2003)
5	NGRDI	Normalized Green-Red Difference Index	RGB	$NGRDI = \frac{G-R}{G+R}$	(Gitelson et al., 2002; Hunt et al., 2005) (Torres-Sánchez et al., 2013)
6	VEG	Vegetation index	RGB	$VEG = \frac{G}{R^{0.667}B^{0.333}}$	(Barbosa et al., 2019; Hague et al., 2006)
7	MExG	Modified Excess Green Index	RGB	$MExG = 1.262G - 0.884R - 0.311B$	(Burgos-Artizzu et al., 2011)
8	COM1	Combined Indices 1	RGB	$COM1 = ExG + CIVE + ExGR + VEG$	(Guijarro et al., 2011)
9	COM2	Combined Indices 2	RGB	$COM2 = 0.36ExG + 0.47CIVE + 0.17VEG$	(Guerrero et al., 2012)
10	NDVI	Normalized difference vegetation index	RGB-NIR	$NDVI = \frac{NIR-R}{NIR+R}$	(Rouse Jr et al., 1974)
11	ECI	Elliptical Color Index	rgb	$ECI = (r - r_0)^2 + (g - g_0)^2/d$	(Lee et al., 2020)
12	TGI	Triangular Greenness Index	RGB	$TGI = G - 0.39R - 0.61B$	(Hunt Jr et al., 2011; Hunt Jr et al., 2013; Fuentes-Penailillo et al., 2018)
13	MGRVI	Modified Green Red Vegetation Index	RGB	$MGRVI = \frac{G^2-R^2}{G^2+R^2}$	(Bendig et al., 2015; Barbosa et al., 2019)
14	RGBVI	Red Green Blue Vegetation Index	RGB	$RGBVI = \frac{G^2-(R*B)}{G^2+(R*B)}$	(Bendig et al., 2015; Barbosa et al., 2019)
15	GLI	Green Leaf Index	RGB	$GLI = \frac{2G-R-B}{2G+R+B}$	(Louhaichi et al., 2001; Barbosa et al., 2019)
16	Hue	Hue	HSV	$\arctan \frac{g-b}{2r-g-b}$	(Yang et al., 2015)

Note. HSV, Hue-saturation-value; NIR, near infrared; rgb, normalized red-green-blue; RGB, red-green-blue.

expensive than COM1 since one fewer component index need be computed.

Our review shows that the CVIs in Table 4 have been utilized in various plant phenotyping areas such as vegetation segmentation. The CVIs used for a specific application critically affect the application performance. However, most of the CVIs were proposed and developed intuitively or empirically without considering the property of pixel distributions. For example, ExG amplifies greenness in vegetation objects by adding the two-color-component differences. In addition,

TABLE 4 Comparison of different color vegetation indices (CVIs) used in comparative studies from the literature. ASMs in the table applies to Authors Segmentation Method(s) (ASM). Best results denote the best SVI except for the ASM

Authors	Vegetation index used	Vegetation species	Best result
Woebbecke et al., 1995	ExG, $r-g$, $g-b$, $(r-g)/(r-g)$, Hue	Cocklebur, velvetleaf	Hue
Meyer & Neto, 2008	ExG, ExGR, NDI	Soybean	ExGR
Golzarian et al., 2012	ExG, g, MEGI, $g-r$, NGRDI, Hue	Wheat, ryegrass, brome grass, fodder oat	Hue
Zheng et al., 2009	ExG, CIVE, ASM[a]	Soybean, weeds	ExG
Zheng et al., 2010	ExGR, NGRDI, CIVE, ASM[a]	Soybean, weeds	Unstable result
Guijarro et al., 2011	ExG, ExGR, CIVE, VEG, COM1	Barley, corn	COM1
Yu et al., 2013	ExG, ExGR, CIVE, VEG, ASM[a]	Maize	ExG
Bai et al., 2013	ExG, ExGR, CIVE, ASM[a]	Rice	CIVE
Guo et al., 2013	ExG,MExG, ExGR, ASM[a]	Wheat	ExGR
Bai et al., 2014	ExG, ExGR, ASM[a]	Rice	ExG
Torres-Sánchez et al., 2014	ExG, ExGR, CIVE, $(g-b)/(r-g)$, NGRDI, VEG, COM1, COM2	Wheat	ExG, VEG
Ye et al., 2015	ExG, NGRDI, CIVE, VEG, ASM[a]	Cotton, corn	CIVE
Barbosa et al., 2019	ExG, NGRDI, VEG, MGVRI, GLI, RGBVI	Emerald grass	NGRDI, MGRVI
Rico-Fernández et al., 2019	ExG, CIVE, VEG, MExG, COM1, COM2	Carrot, maize, tomato	CIVE
Netto et al., 2018	ExG, ExGR, NDI	Maize	NDI, ExGR
Biswas et al., 2020	ExG, ExGR, COM2, GRB, $R-G$, TGI, NDVI	Mangrove trees	ExG
Campos et al., 2016	ExG, ExGR, $Gray_1$, CIVE, VEG, COM1, ASM[a]	Maize	$Gray_1$[b]
Lee et al., 2020	ExG, ExGR, CIVE, VEG, NGRDI, COM1, ECI, Hue	Wheat, three kinds of weeds	ECI
Coy et al., 2016	ExG,CIVE, ASM[a]	Oat, corn, rapeseed, flax	ExG
Montalvo et al., 2016	ExG, ExGR, CIVE, VEG, NDI, COM1, ASM[a]	Maize	COM1
Moorthy et al., 2015	ExG, ExGR, CIVE, ASM[a]	Sugar beet, maize	CIVE
Yang et al., 2015	ExG, ExGR, CIVE, VEG, COM2, Hue	Maize	Hue
Hassanein et al., 2018	ExG, ExGR, NGRDI, Hue, ASM[a]	Soybean, canola, and organic bean	Hue
Zhuang et al., 2018	ExG, RGB, CIVE, ASM[a]	Sugar beet	RGB

Note. CIVE, Color Index of Vegetation Extraction; COM1, Combined Indices 1; COM2, Combined Indices 2; ExG, Excess Green Index; ExGR, Excess Green minus Excess Red; GLI, Green Leaf Index; HSV, Hue-saturation-value; MExG, Modified Excess Green Index; NDI, normalized difference index; NGRDI, Normalized Green-Red Difference Index; NIR, near infrared; RGB, red-green-blue; RGBVI, Red Green Blue Vegetation Index; TGI, Triangular Greenness Index; NDVI, normalized difference vegetation index; VEG, vegetation index.

[a]Denotes a segmentation method suggested by the author.

[b]$Gray_1 = 1.262g - 0.884r - 0.311b$.

NDVI uses the near-infrared (NIR) and red channels in its formula. The healthy vegetation reflects green light and NIR but absorbs blue and red lights. So, NDVI is a way to measure healthy vegetation (Ozyavuz et al., 2015). Furthermore, CIVE, COM1, COM2, and MExG were proposed based on data analysis. These CVIs focused on exploiting the fact that plants are green without any theoretical consideration of CVI function shapes. Therefore, such indices often fail to yield robust performance and adaptability to a wide variety of image conditions. A recent color index, ECI, and notable exception to the previous observation, was proposed and validated by Lee et al. (2020); ECI was mathematically developed based on the discriminant analysis as an ellipse equation with a shape parameter in the *rg* plane. The ECI is a new quadratic type of CVI that is defined by considering the properties of pixel contributions. It was shown that ECI outperforms seven

color CVIs (including ExG, ExGR, CIVE, and COM1) considered in their studies, as shown in Table 4.

It is challenging to definitively recommend a superior CVI for general use because the image datasets used in different comparative studies are not the same. In Table 5, the vegetation species, background, and illumination conditions are considered for six popular CVIs. According to Tables 4 and 5, Hue, ExG, and ExGR are recommended based on the number of times used in comparative research and the high frequency with which they produce best results. Hue color index was used in four comparative studies and tested with the most variable illumination and background conditions while outperforming other indices. According to Table 4, ExG and ExGR are the most popular indices since they appear in many studies and frequently occurs as the best performing indices in comparative studies. Hamuda et al. (2016) showed that ExG is good for addressing shadows and ExGR shows good adaptability in outdoor environments.

Segmenting and extracting vegetation using CVIs have both advantages and disadvantages that have been summarized by Hamuda et al. (2016). The advantages (a) are simple to understand and implement; (b) are easy to modify to create new CVIs; (c) do not require expensive training phases or large image datasets (in contrast to machine learning methods); (d) can perform well over a range of illumination intensities; (e) can, for certain CVIs, achieve comparable results to the state-of-the-art segmentation methods (e.g., Golzarian et al., 2012; Lee et al., 2020; Rico-Fernández et al., 2019); (f) can be designed or images acquired using cameras with any number and type of imaging channels; and (g) are generally suitable for real-time applications using inexpensive hardware for high-throughput phenotyping pipelines. The disadvantages (a) rely on other methods to determine a suitable threshold of the CVI; (b) are generally not effective in applications when the illumination intensity is extremely high or low; and (c) work only for plant segmentation tasks where green is the dominant plant color.

3.1.2 | Threshold-based Approaches

In image processing techniques, segmentation involves separating an image into small regions. Thresholding is the simplest of segmentation methods. Thresholding can be used to generate binary images from grayscale images by setting all pixels below the threshold to a value of 0 and the rest of the pixels to a value of 1. If $f(x,y)$ is a grayscale image (e.g., a feature map computed using a CVI), then $g(x,y)$ is a binary image for some global threshold T:

$$g(x,\ y) = \begin{cases} 1\ if\ f(x,\ y) \geq T;\ and \\ 0\ otherwise. \end{cases}$$

TABLE 5 Comparison of six common and popular color vegetation indices used in comparative studies that obtained the best result

Color-indices	Light conditions	Background conditions	Vegetation species
ExG	Cloudy, sunny, natural sunlight, shaded and unshaded surface, shade,	Corn and wheat residue, ash, light and dark soil, straw background	Mazie, rice, soybean, weeds, wheat, oat, corn, rapeseed, flax, and mangrove trees
ExGR	Sunny, cloudy, sunny with shadows, rainy, natural sunlight at solar noon	Bare clay soil, weathered corn stalk, wheat straw residue	Soybean, wheat, and maize
COM1	Sunny	Soil	Barley and corn
CIVE	Cloudy, sunny, overcast, shade	Light and dark soil	Cotton, corn, rice, sugar beet, carrot, tomato, and maize
Hue	Natural sunlight and shade, cloudy, sunny	Light and dark soil, wheat and corn residue, soil, ash, and straw background	Wheat, ryegrass, bromegrass, fodder oat, Cocklebur, velvetleaf, maize, soybean, canola, organic bean
COM2	Cloudy, sunny	Soil	Maize

Note. CIVE, Color Index of Vegetation Extraction; COM1, Combined Indices 1; COM2, Combined Indices 2; ExG, Excess Green Index; ExGR, Excess Green minus Excess Red.

As mentioned in the previous section, CVI approaches to vegetation segmentation use a global threshold of the CVI to distinguish vegetation from background. Too-low threshold leads to oversegmentation, and a too-high threshold leads to undersegmentation results, thus, selection of the proper threshold for a given image plays a vital role in segmentation.

Due to the importance of choosing the appropriate threshold, some sophisticated approaches have been developed to detect a good threshold for a particular input image.

The advantages and disadvantages of selected automatic threshold detection methods are discussed below.

Otsu's threshold detection method (referred to as Otsu; Otsu, 1979) is widely used to threshold CVI feature maps in vegetation segmentation tasks (Guerrero et al., 2012; Guijarro et al., 2015; Keller et al., 2018; Montalvo et al., 2016; Parraga et al., 2018). The method minimizes the weighted sum of the intraclass variance of the intensity values in the image. The theoretical bases of Otsu's method assumes that the image histogram is bimodal and does not work well when the assumption is violated. Hence this method can fail when image noise obfuscates the histogram modes, when the vegetation area is small compared with the background/soil area (causing the histogram to be largely unimodal), or when the image is not taken under uniform lightening conditions. Kirk et al. (2009) proposed a method that uses a combination of greenness and intensity pixels, which originate from green and red channels under different lighting conditions.

A threshold is selected based on the Gaussian distribution function of pixel intensities. Similar to Otsu's method, the authors assumed that the distribution of pixel intensities can be approximated by two Gaussian distributions and that the vegetation distribution corresponds to the higher-intensity mode. The threshold was determined where the conditional probabilities of soil and vegetation are equal. This method computed two features for each pixel: a greenness feature (g), as the decimal logarithm of the ratio between the red and green pixel values, and a brightness feature, (L), as the difference between the decimal logarithms of the green value and the mean value over the full image. Pixels are classified by projecting the g and L magnitudes onto a one-dimensional axis by applying a rotation angle. The proposed method works well in a various illumination conditions such as overcast, direct sun, and soft sun. However, this method requires the previous estimation of a rotation angle.

Jeon et al. (2011) computed the Normalized Excessive Green index ($2.8 \times g - r - b$) from RGB images. An automatic threshold was automatically determined by finding a value that minimizes the summation of variance between plant and soil pixels. Although the proposed method provides automatic adaptive segmentation, threshold adjustment is required to decrease random noise and plant segmentation error. The threshold value was adjusted by an increment (or decrement) formula when the initial number of segmented pixels was smaller than 0.5% or larger than 20% of total number of image pixels. The increment (or decrement) was determined by the difference between segmented pixels' rate with respect to the total image pixels and lower segmentation limit (0.5%) or upper segmentation limit (20%).

Hassanein et al. (2018) introduced a threshold-based vegetation segmentation method, which depends on the Hue colour channel. Using the HUE histogram of an RGB image, five steps were developed to select five different threshold values to discriminate vegetation from nonvegetation regions in an agriculture field image. First, an RGB image was converted to Hue-saturation-value (HSV) color space. Second, the Hue values with a small number of pixels in the Hue image histogram are removed. The main reason for this step is to work as an outlier remover procedure that remove low importance Hue values. Then, five thresholds were detected based on the highest represented Hue value from the filtered Hue histogram, and Hue value ranges between yellow color at 60° and cyan color at 180°. Finally, the best threshold was applied to the Hue image. If there is no threshold that provides the best segmentation, they considered the average of five threshold values as a satisfactory solution for the suitable threshold value. The proposed method was able to generate accurate vegetation segmentation regardless of the flight height, crop types, growth stages, and illumination conditions. The proposed method outperformed ExG + Otsu, ExGR + Otsu, NGRDI + Otsu, and Hue + Otsu methods, where NGRDI is Normalized Green-Red Difference Index.

Two approaches were proposed based on Gaussian mixture model in 2012 by Liu et al. (2012) and in 2016 by Coy et al. (2016) to segment and estimate plant canopy from background. In these studies, RGB images were converted to CIE La * b * color space. The algorithm used Gaussian mixture model to separate the distribution of the vegetation and background to determine a threshold automatically. One of the limitations of these proposed methods was that when the canopy is close to closure or vegetation is sparse, the bimodal distribution is not apparent, and the method is likely to fail to produce a good threshold. This is especially likely when the background includes weeds or algae.

Li et al. in 2018 proposed the half-Gaussian fitting method for fractional vegetation cover estimation (Li et al., 2018). They used low-altitude remote-sensing UAV images of corn during three growth stages at different flight altitude. In the proposed method, first, RGB images were converted to (CIE) La* b* color space. Then, two half-Gaussian distributions were fit to the histograms of pure vegetation and pure background pixels. Finally, based on Gaussian distribution parameters, a proper threshold was determined to estimate fractional vegetation cover. Compared with the previous studies proposed by Liu et al. and Coy et al. (Liu et al., 2012; Coy et al., 2016), Li et al's method excluded uncertain(mixed) pixels in

the histogram distributed between the bimodal peaks of background and vegetation to avoid negative influence of mixed pixels. In low-resolution low-altitude remote-sensing images, the number of mixed pixels increases. Then, many mixed pixels resulted in weakly bimodal or even unimodal distribution, leading to more error for finding the proper threshold. All three methods obtained similar performance in early-season images because the number of mixed pixels was low. However, the half-Gaussian fitting method for fractional vegetation cover estimation outperformed the other two methods in mid-season and late-season images because the number of mixed pixels increased, which reduced the accuracy of the other two methods.

In summary, the body of work comprising CVI thresholding methods for vegetation segmentation shows that diverse vegetation indices have been used for crop, weed, and general vegetation segmentation. Performance of CVI thresholding usually relies on favorable image background content and non-extreme illumination conditions. CVIs thresholding algorithms must be designed for a specific application and threshold selection adjusted to prevailing illumination conditions to achieve the best performance. None of the CVIs reviewed are robust enough to achieve high performance over all conceivable applications, crops/plants, weather, and imaging conditions.

3.2 | Traditional machine-learning-based approaches

In studies presented by Hamuda et al. (2016) and Tian and Slaughter (1998), the range of daytime light sources may result in noise in the background and poor-quality image, which degrades the segmentation processes. Learning-based vegetation segmentation methods were developed to extract useful information in unstructured lighting conditions. Figure 3 illustrates common variations in the processing pipelines for machine-learning-based methods. Two strategies have been used: (a) using machine learning methods to classify the vegetation pixels; (b) using transformation methods to obtain a threshold for a CVI or a new CVI and extract (non-CVI) features. The majority of methods fall into the first category. A summary of the properties of the learning-based approaches we surveyed is summarized in Table 6.

3.2.1 | Learning to classify thresholded feature maps

This section presents methods that follow the approach of the teal path in Figure 3. Tian and Slaughter (1998) developed an environmentally adaptive segmentation algorithm (EASA) for plant detection in outdoor tomato (*Solanum lycopersicum* L.) fields using normalized RGB color space. The EASA consists of two steps. The first step includes training and learning steps for the image segmentation part. The EASA learns about various illumination conditions, different crops, weeds, and soil types in this step. The second step includes generating a Bayesian classifier and producing a look-up table. A look-up table is a table containing all possible combinations of features measured from the image and label, which specifies the class assigned by the classifier to each combination. Later, Ruiz-Ruiz et al. (2009) applied the EASA with Hue and Hue-saturation (HS) color spaces instead of RGB color space used in the Tian and Slaughter study. This algorithm was developed to achieve real-time processing in sunflower fields. The EASA obtained more efficient vegetation segmentation when plants are in their second or third growing stages (second stage: 4–6 leaves and third stage: 8–10 leaves). Since the EASA relies on segmentation without the intensity component, various illumination conditions did not significantly affect the EASA using different color spaces. The EASA using rgb achieved slightly better segmentation results than both the EASA using HS and Hue. On the other hand, the computation time in processing each image was 25 and 46 times lower for HS and Hue, respectively. The EASA's limitation is that the framing angle should be adjusted to perpendicular to the ground to reduce the effect of shade in case of direct sun illumination.

Bai et al. in 2013 proposed a new color-based crop segmentation method using the morphological modelling method to determine crop color region in the CIE L*a*b* color space (Bai et al., 2013). They applied morphological dilation and erosion to distinguish the crop and background pixels under complicated illumination conditions. This method is robust to the variation of illumination in the agricultural field. However, the improvement of the proposed approach was insignificant by utilizing different structure element sizes in the training phase. This method obtained the mean of segmentation quantities of about 87.2%. Later, Bai et al. in 2014 presented a new vegetation segmentation method in the CIE L*a*b* color space using particle swarm optimization based k-means clustering and morphology modelling (Bai et al., 2014). The method was divided into two stages: offline learning and online segmentation. The optimal clustering number and the vegetation color model through morphological modeling were obtained in the offline stage. The online segmentation stage particle swarm optimization based on k-means clustering was utilized to separate the pixels in vegetation and nonvegetation classes. The accuracy of this method was about 88.1 and 91.7 for rice (*Oryza* L.) and cotton (*Gossypium* L.), respectively. This method is robust to segment vegetation in the various illumination conditions. Nonetheless, this algorithm was not suitable for real-time applications but also suffered from long run time and depends on many processing steps.

TABLE 6 Comparison of learning-based segmentation approaches

References	Method	Description	Method's strategy	Color spaces	Advantages	Limitations
(Tian & Slaughter, 1998)	EASA	Environmentally adaptive segmentation algorithm	Classify pixels	RGB	1. Various illumination conditions did not significantly affect the EASA using different colour spaces. 2. The EASA using rgb achieved slightly better segmentation results.	1. It requires sufficient training data to obtain good segmentation results 2) The framing angle should be adjusted to reduce the effect of shade in case of direct sun illumination.
(Ruiz-Ruiz et al., 2009)	EASA	Environmentally adaptive segmentation algorithm	Classify pixels	HSV	The computation time is lower for HSV color space	EASA is not effective to segment plants at early growing stage
(Zheng et al., 2009)	Mean-shift	Mean-shift algorithm with back propagation neural network (MS-BPNN)	Classify pixels	RGB and HSI	Obtain a good performance in different images under various illumination conditions	1. Obtain a low performance for green vegetation regions with shadows. 2. Suffers from the high computation time
(Zheng et al., 2010)	Mean-shift	Mean-shift algorithm with Fisher linear discriminant (MS-FLD)	Classify pixels	LUV	Obtain better segmentation performance on green parts with shadow and without shadows	Suffers from high computation time
(Guerrero et al., 2012)	SVM	Support vector machine	Classify pixels	RGB	Able to identify weeds and crops	Relies on the results obtained from other steps such as color-index and thresholding step
(Rico-Fernández et al., 2019)	SVM	Support vector machine	Classify pixels	CELuv	Segments vegetation in various environments and crop species	
(Guo et al., 2013)	DTSM	Decision based segmentation model	Classify pixels	RGB, YCbCr, HSV, CIEL*a*b, and CIEL*u*v	Requires no threshold adjustment for each image	Relies on training data and needs further improvement to use it practically

(Continues)

TABLE 6 (Continued)

References	Method	Description	Method's strategy	Color spaces	Advantages	Limitations
(Yu et al., 2013)	AP-HI	Affinity propagation-hue intensity	Classify pixels	HSI	Obtain great segmentation result from a small number of training samples with an accuracy of 96.68%	The choice of threshold in the HSI color model and the classification step is crucial for segmentation.
Bai et al. (2013), (2014)	PSO	Particle Swarm Optimisation Clustering and Morphology Modelling	Classify pixels	CIEL*a*b	Robust to segment vegetation in the various illumination conditions	Suffers from long run time and depends on many processing steps.
(Sadeghi-Tehran et al., 2017)	MFL	Multifeature Learning	Classify pixels	RGB, YCbCr, HSV, HSI, CIEL*a*b, and CIEL*u*v	1. Able to segment vegetation in various environments with different illumination conditions 2. Does not need adjusting threshold for each image	Labelling a wide range of training samples is time-consuming
(Zhuang et al., 2020)	MCMFL	Multiclass and multifeature learning	Finding a threshold	RGB, HSV, CIEL*a*b	1. Able to extract vegetation with efficient performance 2. Implement real-time plant segmentation	Suffers from long run time.
(Montalvo et al., 2016)	PCA	Principal component analysis	Finding a threshold	RGB	1. Obtain a new index called index principal component analysis (IPCA). 2. Achieves a better measure of an image's greenness than simple indices, with an error rate of 8.07%.	Other processes are needed, such as color space transformation when the color difference between plants and weeds is not significant.

(Continues)

TABLE 6 (Continued)

References	Method	Description	Method's strategy	Color spaces	Advantages	Limitations
(Montalvo et al., 2018)	PCA	Principal component analysis	Finding a new color index	RGB	1. Outperforms five indices followed by Otsu or mean thresholding methods with 98% success. 2. Capture the most significant information to improve the segmentation.	Relies on previous steps (Threshold).
(Guijarro et al., 2015)	DWT	Discrete Wavelet Transform	Extract more features	RGB	1. Combine greenness and spatial texture information to segment plants from the soil. 2. Outperforms existing binarization approaches such as Otsu, COM, SVM with a lower average error of 7.12%.	Depends on the sensor used for capturing the images.
(Arroyo et al., 2016)	KNN	K-nearest Neighbors	Finding an automatic threshold	RGB	Able to detect the plant from the soil under different illumination conditions and various stages of plant growth.	It requires to prepare a specific and careful dataset
(Campos et al., 2016)	BoW SVM	Bag of word support vector machine	Classify pixels	RGB	1. Achieves good performance over 95% accuracy. 2. outperforms color-indices	Relies on obtaining the regions of interest

Note. AP-HI, affinity propagation-hue intensity; DTSM, Decision Based Segmentation Model; DWT, Discrete Wavelet Transform; EASA, environmentally adaptive segmentation algorithm; HSI, Hue-saturation-intensity; HSV, HSV, Hue-saturation-value; RGB, red-green-blue.

Guerrero et al. (2012) proposed a method based on the support vector machine (SVM) to classify masked (soil and other materials) and unmasked plant regions in the maize field. This method consists of learning and decision phases. The learning phase consists of several steps. First, a binary image, which determines two classes, was obtained by calculating the COM1 color-index followed by the Otsu thresholding method. Then, support vectors associated with each class were identified based on SVM. In the decision phase, a new image containing masked and unmasked plants was given to the algorithm to identify pixels that belong to each class. As sometimes plants have been contaminated with materials coming from the soil due to natural rainfall or artificial irrigation, this method was able to identify weeds and crops. However, this method relies on the results obtained from other steps such as color-index and thresholding step. In another study, Rico-Fernández et al. (2019) proposed a vegetation segmentation approach that could be applied in various crops. In this method, authors transformed RGB color space to CIEL*u*v color space. Then, they generated the SVM classifier to classify pixels into plant or nonplant. Using this approach, the authors performed segmentation in various environments and crop species.

Campos et al. (2016) proposed a methodology for vegetation segmentation in cornfield images. They adapted a bag-of-word method originally designed to extract features from text documents to computer vision applications (Crnic, 2011). In this study, the proposed method included two main steps: a low-level segmentation process to obtain the region of interest (ROI) and a class label assignment using a bag-of-word method. In the first stage, an SVM classifier was designed to model for three classes of vegetation, soil, and others. In the second stage, the classifier was used to predict the label of a new ROI. This method achieved good performance over 95% accuracy and outperformed CVI methods. However, the proposed method relies on obtaining the ROIs because the results showed that different segmentation methods for obtaining ROIs resulted in different performances.

Guo et al. (2013) proposed a method to extract vegetation regions from the background in wheat images taken under natural light conditions. They created 18 color features from six common color spaces (rgb, YCbCr, HSV, CIEL*a*b*, and CIEL*u*v*). Then, a decision tree model was generated using the classification and regression trees classifier (Breiman et al., 1984). This method not only was able to address the illumination problem, such as shadow and specularly reflected regions, but also required no threshold adjustment for each image. However, this method needs further improvement to use practically because its accuracy remained around 0.8.

Yu et al. (2013) designed a new segmentation algorithm that combined the Hue-intensity (HI) look-up table and affinity propagation (AP) clustering method to extract maize plants from background. The AP algorithm was applied to cluster pixels by maximizing the similarity of colors in each class. Later, the HI color model was used to judge each class taking into consideration the distribution parameters (expectation and variance) of the Gaussian distribution of the hue of green in certain intensity. This work can produce a great segmentation result from a small number of training samples while meeting the actual field environment's requirements with an accuracy of 96.68%. The AP-HI outperformed the EASA (Tian & Slaughter, 1998) and the other four CVI thresholding methods. However, this method misclassified vegetation areas during daylight where some parts of the maize plant reflected the light (highlighted areas).

Zheng et al. (2009)proposed an algorithm to improve the vegetation segmentation using the mean-shift algorithm with back-propagation neural network (MS-BPNN). In the first step, six features were extracted for each pixel—$G - R$, $G - B$, H, S, x, and y—where x and y are pixel positions, and H and S are hue and saturation from the Hue-saturation-intensity (HSI) color space. Then, the mean shift procedure and a back propagation neural network (BPNN) were employed to complete crop image segmentation algorithm. MS-BPNN obtained a good performance in different images under various illumination conditions compared with several CVI thresholding method but performed poorly on green vegetation regions with shadows. MS-BPNN also suffers from high computation time due to the use of the mean shift algorithm. In other studies published in 2010 by Zheng et al., a hybrid method of combined mean-shift with the Fisher linear discriminant (FLD) was proposed. In this study, the FLD was replaced with BPNN and the Luv colour space replaced the RGB and HSI color spaces. Compared with the algorithm in Zheng et al. (2009) and several CVI thresholding, the mean-shift algorithm with Fisher linear discriminant (MS-FLD) achieved a high-quality performance on the green vegetation regions with or without shadows. However, the MS-FLD, like the MS-BPNN, suffers from a long time run.

Sadeghi-Tehran et al. (2017) proposed a multifeature learning model (MFL). The method was represented in two stages, offline training and online segmentation stages. First, the authors generated vegetation and background patches manually labelled from wheat images. Then, 21 features from seven color spaces (RGB, YCbCr, HSV, HSI, YUV, CIEL*a*b*, and CIEL*u*v*) were extracted to be used to describe different properties of an image. Next, the random forest classifier was used to train the model (Ho, 1998). In the next stage, testing sample images were given to the model and classified as vegetation and or background classes to generate a binary image. Finally, a median filter was applied to minimize the noise. This method is not only able to segment vegetation in various environments with different illumination conditions but also does not need an adjusting threshold for each image. The proposed method outperformed several CVI

thresholding methods and k-means clustering algorithms. However, labeling a wide range of training samples is time-consuming.

Zhuang et al. proposed a method to extract vegetation in the field using the multiclass and multilevel features method (Zhuang et al., 2020). Two datasets were used, which contain strong and weak light illuminations, shadow regions, cloudy, overcast, and rainy days, and night field conditions. The proposed method included four steps: re-labeling the training samples, extracting multilevel features, training the logistic regression model, and evaluating the testing dataset. It can extract vegetation with efficient performance and implement real-time plant segmentation for automatic agriculture applications in the fields. The proposed multiclass and multilevel features method achieved good performance over 96% and outperformed MFL (Sadeghi-Tehran et al., 2017), SVM classifier, and two CVI thresholding methods.

3.2.2 | Using Transformation techniques to obtain a Threshold for a CVI or a new CVI and extract (non-CVI) Features

This section presents methods that follow the approach of the dotted purple path in Figure 3.

Montalvo et al. (2016) proposed a vegetation segmentation method based on principal component analysis (PCA). This method included two automatic stages, the segmentation phase, and the thresholding phase. Five color vegetation indices were calculated in the first stage: ExG, ExGR, normalized difference index (NDI), CIVE, and VEG. Then, a new index was created by combining five indices using the PCA method into a new index called index principal component analysis (IPCA). The main advantage of the study is that IPCA achieved a better measure of an image's greenness than simple indices, with an error rate of 8.07%. In another study by Montalvo et al. (2018), a method was developed to detect green plants in a maize crop. This method was based on five main steps: segmentation, dimensionality reduction using PCA, Otsu thresholding, threshold combination, and final thresholding. As in the earlier research of this author, PCA was used to combine several indices to extract the image's greenness. A threshold was obtained by combining the Otsu thresholds of the basic vegetative index images using the PCA weights. This method had been compared with the standard Otsu method and the mean thresholding of ExG, ExGR, CIVE, VEG, and NDI indices. The new method outperformed using any of the five indices followed by Otsu or mean thresholding methods, having 98% success due to capturing the most significant information to achieve the segmentation.

Arroyo et al. (2016) proposed a k-nearest neighbor algorithm for the segmentation of crop images. In this study, images were represented by their ExG histograms. Then, all histograms were stored with their correct threshold that discriminates plant regions from the background. Finally, k-nearest neighbor methods were used to adapt histogram data to the automatic thresholding of images. The proposed method is able to detect the plant from the soil under different illumination conditions and various stages of plant growth. However, this method needs to prepare a specific and careful dataset to be used for the selection of the nearest neighbours. The method also requires a constrained environment, such as a similar camera angle and crop.

Guijarro et al. (2015) presented a vegetation segmentation method that combined greenness and texture spatial information through the wavelet transform to discriminate plant and soil parts. This method consists of five steps. In the first step, the ExG color index was obtained from the RGB color space. Four down-sampled images containing approximation coefficient and horizontal, vertical, and diagonal details coefficients were obtained using a wavelet-based decomposition. The authors then modified the pixels in the approximation coefficient to new greenness value by computing the standard deviation for each detail coefficient. Next, the authors applied an inverse discrete wavelet transform with new approximation coefficient to obtain an improved ExG image with improved greenness information. Finally, the Otsu approach was used to obtain a binary image. This approach's main advantages are that the proposed method combined greenness and spatial texture information to segment plants from the soil. As the green part and soil have irregular spatial texture distribution, wavelet decomposition provides important vegetation segmentation improvements. The Discrete Wavelet Transform separates low-frequency components of the image (slight greenness variations) from high-frequency components (edges and high variability that give more detail) to extract spatial structures in three bands while preserving the original information.

According to the studies reviewed in this section, learning-based approaches demonstrated the best vegetation segmentation performance compared with CVI-thresholding methods under various illumination conditions because they rely on the training step. A direct comparison of learning-based approaches is challenging as different datasets have been used in comparative studies. A summary of the experimental conditions of the learning-based approaches we surveyed is summarized in Table 7. According to Table 7, the most approaches were compared with CVIs methods. However, some methods were improved by the same authors compared with their previous approaches, such as studies published by Bai et al. (2014) and Zheng et al. (2010). Two papers proposed by Bai et al. (2014) and Bai et al. (2013) are comparable because the dataset and accuracy metrics are the same. Furthermore, to evaluate the performance of algorithms, some methods employ other algorithms on their datasets with the same evaluation metrics (e.g., Zhuang et al., 2020; Bai et al., 2014; Bai et al., 2013; Yu et al., 2013; Guijarro et al., 2015; Zhuang et al.,

TABLE 7 Experimental conditions of learning-based segmentation studies

Studies	Methods	Datasets	Evaluation metrics	Compared results with
Tian and Slaughter (1998)	EASA-RGB	Tomato images	F value	OSM[a]
Ruiz-Ruiz et al. (2009)	EASA-HSV	Sunflower images	False Positives (FP) and False Negative (FN) Rates	EASA-RGB(Tian & Slaughter, 1998)
Zheng et al. (2009)	MS-BPNN	20 Soybean images, and 80 images covered five soil types, and 40 Weed Images	The median (Med), Max and Min of the mis-segmentation of green vegetation and background region	ExG and CIVE
Zheng et al. (2010)	MS-FLD	50 soybean images, 20 weed images	The Means of Segmentation Qualities, $Q = \frac{\lvert A \cap B \rvert}{\lvert A \cup B \rvert}$	MS-BPNN, ExGR, NDI, and CIVE
Guerrero et al. (2012)		70 maize images	Averaged values for the green spectral components, standard deviations, ratios, and tolerances of green.	–
Rico-Fernández et al. (2019)	SVM	The tomato, carrot, maize datasets	$Qseg = \frac{\lvert A \cap B \rvert}{\lvert A \cup B \rvert}$	ExG, ExGR, CIVE, MExG, COM1, COM2, CIE Luv+SVM, and CIVE+SVM
Guo et al. (2013)	DTSM	Wheat plant images	$Qseg = \frac{\lvert A \cap B \rvert}{\lvert A \cup B \rvert}$	ExG, ExG-ExR, and MExG
Yu et al. (2013)	AP-HP	50 maize images	$Qseg = \frac{\lvert A \cap B \rvert}{\lvert A \cup B \rvert}$	ExG, VEG, CIVE, ExGR, EASA-RGB (Tian & Slaughter, 1998)
Bai et al. (2013)	PSO	Rice images	The Means of Segmentation Qualities, $Qseg = \frac{\lvert A \cap B \rvert}{\lvert A \cup B \rvert}$	ExG-Otsu, ExGR, CIVE EASA-RGB (Tian & Slaughter, 1998) and OSM[a], AP-HI (Yu et al., 2013)
Bai et al. (2014)	PSO	Rice and cotton images	The Means of Segmentation Qualities, $Qseg = \frac{\lvert A \cap B \rvert}{\lvert A \cup B \rvert}$	ExG-Otsu, ExGR, EASA-RGB(Tian & Slaughter, 1998), AP-HI (Yu et al., 2013), and OSM[a]
Sadeghi-Tehran et al. (2017)	MFL	Six wheat images	Qseg and Error Rate	ExG, ExGR, CIVE, and OSM[a]

(Continues)

TABLE 7 (Continued)

Studies	Methods	Datasets	Evaluation metrics	Compared results with
Zhuang et al. (2020)	MCMFL	Image collected from the Internet and published studied (Chebrolu et al., 2017; Lu et al., 2016)	$Qseg = \frac{\lvert A \cap B \rvert}{\lvert A \cup B \rvert}$	ExGR, COM1, MFL (Sadeghi-Tehran et al., 2017), SVM (Guerrero et al. (2012)), and OSM[a]
Montalvo et al. (2016)	PCA	Maize crops	Error Rate	ExGR, ExG, VEG, NDI, and COM1
Montalvo et al. (2018)	PCA	Maize crops	False Positives (FP), False Negative (FN), and Error Rates	ExGR, ExG, VEG, and NDI
Guijarro et al. (2015)	DWT	1200 maize images	Precision, Recall, and Accuracy	ExG, COM1, OSM[a], and SVM (Guerrero et al. (2012))
Arroyo et al. (2016)	KNN	Maize images	The mean absolute error (MAE) and misclassification Rate	OSM[a]
Campos et al. (2016)	BoW-SVM	Maize plants	False Positives Rate (FP), False Negative Rate (FN), Positive predictive value (PPV), Negative predictive value (NPV), and F-measure	ExG, ExGR, CIVE, VEG, Gray1, and OSM[a]

Note. AP-HP, affinity propagation-hue intensity; BoW-SVM, bag of word support vector machine; CIVE, Color Index of Vegetation Extraction; COM1, Combined Indices 1; COM2, Combined Indices 2; DTSM, Decision Based Segmentation Model; DWT, Discrete Wavelet Transform; EASA, environmentally adaptive segmentation algorithm; ExG, Excess Green Index; ExGR, Excess Green minus Excess Red; GLI, Green Leaf Index; HSV, Hue-saturation-value; KNN, k-nearest neighbour; MCMFL, multiclass and multifeature learning; MExG, Modified Excess Green Index; MFL, multifeature learning; NDI, normalized difference index; NGRDI, Normalized Green-Red Difference Index; NIR, near infrared; PCA, principle component analysis; PSO, particle swarm optimization; RGB, red, green, blue; SVM, support vector machine; TGI, Triangular Greenness Index; NDVI, normalized difference vegetation index; VEG, vegetation index.

[a]Denotes other segmentation methods (OSMs) that do not review in the survey paper.

2020). These papers might be comparable because they used the same dataset and the evaluation metrics to interpret their outcomes.

3.3 | Deep-learning-based approaches

In this section, we discuss the research efforts that employ deep learning techniques applied to various agricultural challenges. The motivation for preparing this section is that deep learning applications in agriculture are recent, modern with promising results, while advancements and applications of deep learning in other domains indicate its large potential (Kamilaris & Prenafeta-Boldú, 2018). Kamilaris and Prenafeta-Boldú (2018) listed a survey of 40 research papers that employed deep learning techniques applied in various agricultural challenges.

3.3.1 | U-Net

U-Net, proposed by Ronneberger et al. in 2015, achieved a much more effective segmentation result and won the ISBI cell tracking challenge. The contracting path or down-sampling layers of U-Net architecture learns the feature maps using alternating convolutional filters and max pooling layers. The expanding path or up-sampling layers act as input for the deconvolution process and provide precise segmentation.

Tausen et al. (2020) developed the Greentyper image analysis pipeline. The proposed method was divided into three sections; the camera system, the image analysis pipeline, the experimental setup. The image analysis pipeline was divided into three steps. First, the authors did some preprocessing tasks, such as color correction and object detection. Then, U-Net was used to perform plant segmentation. Finally, post-processing steps were applied to produce the final predicted masks. The image analysis pipeline was robust under different greenhouse conditions, such as overlapping and unpredictable growth patterns and different plant locations. The author concluded that the proposed method provides reliable detection of plant area when there are multiple plants in the same image. The proposed method facilitates future large-scale studies as the method is used as a guide for developing large and complex experiment pipelines in image analysis.

3.3.2 | DeepLabV3+

DeepLab was a state-of-the-art architecture open-sourced by Google in 2016 (Chen et al., 2017). It has iteratively been improved upon in subsequent DeepLab V2, DeepLab V3, and the latest DeepLab V3+ architectures (Chen et al., 2017). The DeepLab model addresses some semantic segmentation challenges using Atrous convolutions and Atrous Spatial Pyramid Pooling modules.

Morales et al. (2018) proposed a semantic segmentation based on DeepLabV3+ architecture to segment Palm trees in aerial images under different environment and illumination conditions. They used 25,248 image patches of 512×512 pixels. This method achieved very good performance (98.036%) accuracy. Compared with four other networks based on the U-Net structure, the proposed model achieved comparable results while having a substantially lower number of trainable parameters. Furthermore, the authors proved that Atrous separable convolution can reduce the computation time compared with regular convolution.

3.3.3 | Deep convolutional neural network (DCNN)

Zhuang et al. (2018) proposed a semantic segmentation approach with fully-convolutional networks to extract green vegetation from the background in different light and weather conditions, such as cloudy, rainy, night, shadow, high light, and weak light. The proposed architecture consisted of two parts, down-sampling and up-sampling, inspired by the VGG16 architecture. Different color indices such as RGB, ExG, and CIVE were used as input for the network, resulting in three networks: RGB-DCNN, ExG-DCNN, and CIVE-DCNN. The performance of these networks were compared with each other and with threhsolding of ExG and CIVE feature maps. The RGB-DCNN obtained a Dice coefficient score of 89.9% and average precision of 89.7%. The RGB-DCNN outperformed ExG-DCNN and CIVE-DCNN and was suitable for real-time crop segmentation applications in the agricultural field.

3.3.4 | SegNet

SegNet, proposed by Badrinarayanan et al. in 2017, is a deep convolutional encoder-decoder network followed by a pixel-wise classification layer. The encoder part of SegNet architecture is based on VGG-16 as a feature extractor. The encoder uses fewer trainable parameters that make the architecture less intensive on memory.

Milioto et al. (2018) proposed a convolutional neural network (CNN)-based semantic segmentation method to extract sugar beet plants and weed from the background. The proposed DCNN network was based on an end-to-end encoder–decoder semantic segmentation network. The authors designed an architecture inspired by SegNet (Bhandari et al., 2015) and Enet. The authors used 14 channels per image including (R, G, B, ExG, ExR, CIVE, NDI, H, S, V, Sobel derivatives in x-direction on ExG, Sobel derivatives in

the y-direction on ExG, the Laplacian on ExG, and Canny edge detector on ExG) to solve the problem of limited training data. The proposed architecture could better generalize to new crops despite the limited training data. The authors implemented and evaluated their proposed method on a real agriculture robot using data obtained from different cities in Germany and Switzerland.

In another study, Fuentes-Pacheco et al. (2019) presented a CNN architecture with an encoder–decoder inspired by SegNet architecture that classifies each pixel into crop or background using RGB images as input. They used a dataset consisting of 110 RGB images classified into five categories: lighting, weeds, soil color, camouflaged plants, and residues. The proposed CNN architecture consists of only seven convolutional layers in both the encoder and the decoder parts. They used fewer convolutional layers in comparison to SegNet with a small number of trainable parameters. This architecture was suitable for two-class segmentation problems.

Generally, deep-learning-based methods outperform traditional machine-learning-based, vegetation-index-based thresholding methods. However, the limited availability of open datasets in the vegetation segmentation area and limited training samples are shortcomings of deep-learning-based methods.

4 | SEGMENTATION OF MICROPLOTS IN AERIAL AGRICULTURE IMAGES

4.1 | Microplot segmentation

Analysis of aerial imagery can accurately assess agricultural field experiments for advancing high-throughput phenotyping (Chen & Zhang, 2020). Current methods require intensive manual operations to segment and identify microplots, which is difficult and time-consuming. Automated identification of field microplots in imagery would allow a faster process that requires fewer person-hours than manual assessment and facilitate automatic monitoring and quantification of microplot phenotypes. Traits extracted from the microplots can explain the plants' coverage, growth, flowering status, and related phenomena. An important prerequisite step to obtain such information is to find the exact position of each microplot from an orthomosaic image. Segmentation of microplots using tools that assume a uniform spacing can be erroneous because the microplots may neither be perfectly aligned nor equally distributed in a field.

There are three types of methods used to extract microplots from orthomosaic images: manual methods (discussed in section 4.1.1), semi-automatic methods (discussed in section 4.1.2), and automatic methods (section 4.1.3). A summary of the automatic and semi-automatic microplot segmentation methods, highlighting their primary limitations, is summarized in Table 8. Since one of the primary and important parts of the preprocessing step in segmenting microplots is vegetation segmentation, we summarized each study's vegetation segmentation strategy in Table 8.

4.1.1 | Manual methods

The manual method localizes a microplot using the geolocation information on the drone to generate bounding boxes. A simple grid-based method to extract microplots was proposed by Haghighattalab et al. (2016). The number of rows and columns of microplots, height, and width of each microplot can be defined by the user. The microplot boundary size can be manually extended by supplying both the minimum and maximum x and y coordinates. This method was developed based on the assumption of a fixed microplot boundary size. However, the microplot boundary may overlap part of its neighbors. The implementation of this method is easy and fast, but it did not account for gaps between microplots and between each range of microplots.

A method to extract microplots based on their map coordinates was proposed by Hearst and Cherkauer (2015). They divided orthomosaic images into microplots using the geolocation information of orthomosaic images. This method depended on accuracy of the geolocation information and used Ground Control Points. Their results could be affected if there is only a narrow gap between microplots or when plants in the later stages of growth obscure the spaces between microplots.

4.1.2 | Semi-automatic methods

Semi-automatic methods require some manual inputs, but much of the work is done by an automatically operating phase. Recio et al. (2013) developed a semi-automatic segmentation method using the K-means classification algorithm to classify image pixels into "tree" and "non-tree" groups. In this method, images were preprocessed by applying Laplacian filter to facilitate the tree extraction process. The limitation of this approach is that they assume ideal separation between microplots and sometimes merge multiple microplots into a single microplot.

Haghighattalab et al. proposed a semi-automatic method to extract microplots from wheat images (Haghighattalab et al., 2016). They first extracted Green normalized difference vegetation index (GNDVI) from orthomosaic images to provide higher intensity value of vegetation than background. Their semi-automatic algorithm localizes microplots by classifying pixels of images into "vegetation"' and "soil" areas. However, this approach requires postprocessing and manual editing to

TABLE 8 Comparison of automatic and semi-automatic microplot segmentation approaches

Author and year	Method	Microplot layout /description	Vegetation/plant segmentation method	Computational language	Limitations
Recio et al. (2013)	K-means Classification	Nonrectangular-shaped/automatic	Laplacian Filter	ArcGIS 10 Software	Ideal separation was assumed between trees; multiple microplots may be seen as a single microplot
Haghighattalab et al. (2016)	Maximum Likelihood Classification	Rectangular-shaped/semi-automatic	GNDVI	Python	Ideal separation was assumed between microplots; multiple microplots may be seen as a single microplot
Parraga et al. (2018)	Image Processing Techniques	Rectangular-shaped/automatic	mExG, NDVI/Otsu threshold	Python	Needs tuning several variables to work for all images; it suffers from long run time
Khan and Miklavic (2019)	Particle Swarm Optimization (PSO)	Rectangular-shaped/semi-automatic	RGB/Otsu threshold	MATLAB R2018b	Requires the software tools to specify the complete spatial characteristics of the grid and approximate alignment in advance
Tresch et al. (2019)	Easy MPE	Rectangular-shaped/semi-automatic	ExG/Otsu threshold	Python	Rely upon the presence of well-spaced plants; the Easy MPE code needs to be further tested and improved by applying it to other crops
Ahmed et al. (2019)	Blob Detection Random Walker K-means Clustering	Nonrectangular-shaped/automatic	NDVI, GNDVI	Python	Rely upon the presence of well-spaced plants
Ribera Prat (2019)	Constrained Optimization by Linear Approximation (COBYLA)	Rectangular-shaped/semi-automatic	HSV/Thresholding H Channel	Python	Equal separation was assumed between microplots; works for mid-season images

(Continues)

TABLE 8 (Continued)

Author and year	Method	Microplot layout /description	Vegetation/plant segmentation method	Computational language	Limitations
Chen and Zhang (2020)	GReenfield Image Decoder (GRID)	Rectangular-shaped and Rhombus-shaped/semi-automatic	Red and NIR channels or Red and Green Channels/K-means Clustering	Python	Unable to distinguish POI regions if weeds are nearly identical to the vegetation of interest; GRID invalidated for other multispectral channels except RGB
Matias et al. (2020)	FIELDimageR	Rectangular-shaped/semi-automatic	NDVI, NDRE	R Package	Rely upon the presence of well-spaced plants
Robb et al. (2020)	Canny Edge Detection, Hough Line Detection, Active Contour	Rectangular-shaped/semi-automatic	RGB	Python	Requires the tuning of edge parameter
Yang et al. (2021)	Comb Function Optimization Plot Extraction (COPE)	Rectangular-shaped/semi-automatic	HSV/Thresholding H Channel	Not mentioned	Ideal separation was assumed between microplots
Mardanisamani et al. (2021)	Three-step image-based optimization technique	Rectangular-shaped/automatic	ExGR, NDVI	Python	Hyperparameter tuning on the whole dataset is quite time-consuming

Note. ExG, Excess Green Index; ExGr, ExGR, Excess Green minus Excess Red; GNDVI, Green normalized difference vegetation index; HSV, Hue-saturation-value; MExG, Modified Excess Green Index; MPE, MicroPlot Extraction; NDVI, normalized difference vegetation index; NDRE, normalized difference red edge index; NIR, near infrared; POI, pixel of interest; RGB, red-green-blue.

clean up the final results because this approach did not separate microplots properly.

Khan and Miklavic proposed a semi-automated approach to extract microplots from wheat field orthomosaic images (Khan & Miklavcic, 2019). This approach consists of two phases. In the first phase, a software tool manually created a grid of rectangular cells based on rows and columns numbers and used a CVI thresholding method to segment vegetation. In the second phase, the authors used particle swarm optimization to automatically find the optimal alignment of a bounding box grid by both calculating the level of vegetation inside a box and the degree of overlapping vegetation with the neighbouring boxes. Their trial image had single-row microplots being inherently misaligned due to variability in sowing position, and validation images had a randomized split-block design of microplots where the microplots had a distinct placement. Their semi-automatic method has several drawbacks. This method used external software to obtain the grid's position and attributes, making the method semi-automatic. In addition, many crops and field-trial layouts require monitoring of the complete growing season from early stages to later stages of growth with little to no visible ground between microplots. However, based on examination on Figure 13 in their paper, it appears as though this method works for early and mid-season images. Because it requires a proper level of vegetation inside a box and visible distance between microplots to determine the optimal microplot position.

Tresch et al. (2019) proposed a microplot extraction method known as Easy MPE (MicroPlot Extraction) to extract microplot information for drone imagery of whole orthomosaic image of a field. This method has four major steps: vegetation segmentation, microplot extraction, shapeFile generation, and reverse calculation. In the first step, the ROI in the orthomosaic was manually selected and CVI thresholding was used to segment vegetation. Then, binary images were segmented into crop rows and columns to extract microplots. Finally, shapefile production and reverse calculation were produced using coordinates obtained during the previous step. The proposed method was able to identify crop rows and columns in soybean and sugarbeet crops on six different field datasets. However, based on examination on Figure 4 in their paper, it appears as though their method was designed for mid-season images when a visible gap between microplots exists. Their method might not work for later-season images in which there is no visible gap between microplots because plants are larger. In addition, Chen and Zhang (2020) reference observed that microplots are often misaligned between rows in their study.

Ribera Prat (2019) proposed a method to extract microplots from UAV images. In the first step, the ROI in the orthomosaic was manually selected. Then, the authors obtained the binary plant segmentation images using thresholding the hue channel from HSV colour space. Finally, the boundary of microplots was found using constrained optimization by linear approximation. However, based on examination on Figure 2.12 in their studies, it appears as though they assume equally spaced between microplots within a row/range. In addition, this method works for mid-season images where there is visible soil between microplots.

Similarly, Yang et al. (2021) developed a tool called Comb Function Optimization Plot Extraction for microplot extraction in RGB orthomosaic images. The method consisted of three main steps: vegetation segmentation using CVI thresholding method, energy function generation, and row and range separation. The authors experimented with the tool on a dataset obtained from maize and sorghum fields at different dates and heights. Their method outperformed Easy MPE (Tresch et al., 2019) and Ribera Prat et al.'s method (Ribera Prat, 2019) in terms of Intersection over Union while also achieving the least amount of manual adjustment time (manual microplot boundary adjustment is needed to correct boundary errors of the segmented microplot). However, based on examination on Figure 15 in their studies, it appears as though their method obtained better results just for early-season images where the fields were planted rectangular-shaped.

Chen and Zhang developed GRID (GReenfield Image Decoder), a Python package, to segment microplots (Chen & Zhang, 2020). The proposed package required an image and an optional map file, representing the identification of microplots arranged in rows and columns as input data. The red and NIR channel or the red and green channels are used in a vegetation segmentation step to identify pixels of interest (POIs) and background. Due to automatically inferring the layout from the image, GRID was able to work without the map file. GRID is a user-friendly Python package that automatically segments microplots from the orthomosaic image with minimal human involvement. GRID was able to obtain better performance compared with other software programs with higher computing time. In addition, GRID can detect different field layouts, such as microplots arranged in rhombus or grid. The authors acknowledge that this tool has some limitations. First, GRID uses RGB channels to control noise and shade, and the users are limited to choosing these channels and cannot use images that capture other wavelengths. Second, GRID is unable to distinguish identifying POI regions if weeds are nearly identical to the vegetation of interest.

Matias et al. developed a user-friendly software to analyze many microplots in orthomosaic images called FIELDimageR (Matias et al., 2020). FIELDimageR segments vegetation using NDVI and normalized difference red edge indices and cropping the microplot area by having a user manually click the four corner points. Then, the cropped region is evenly divided into microplots based on the number of rows and

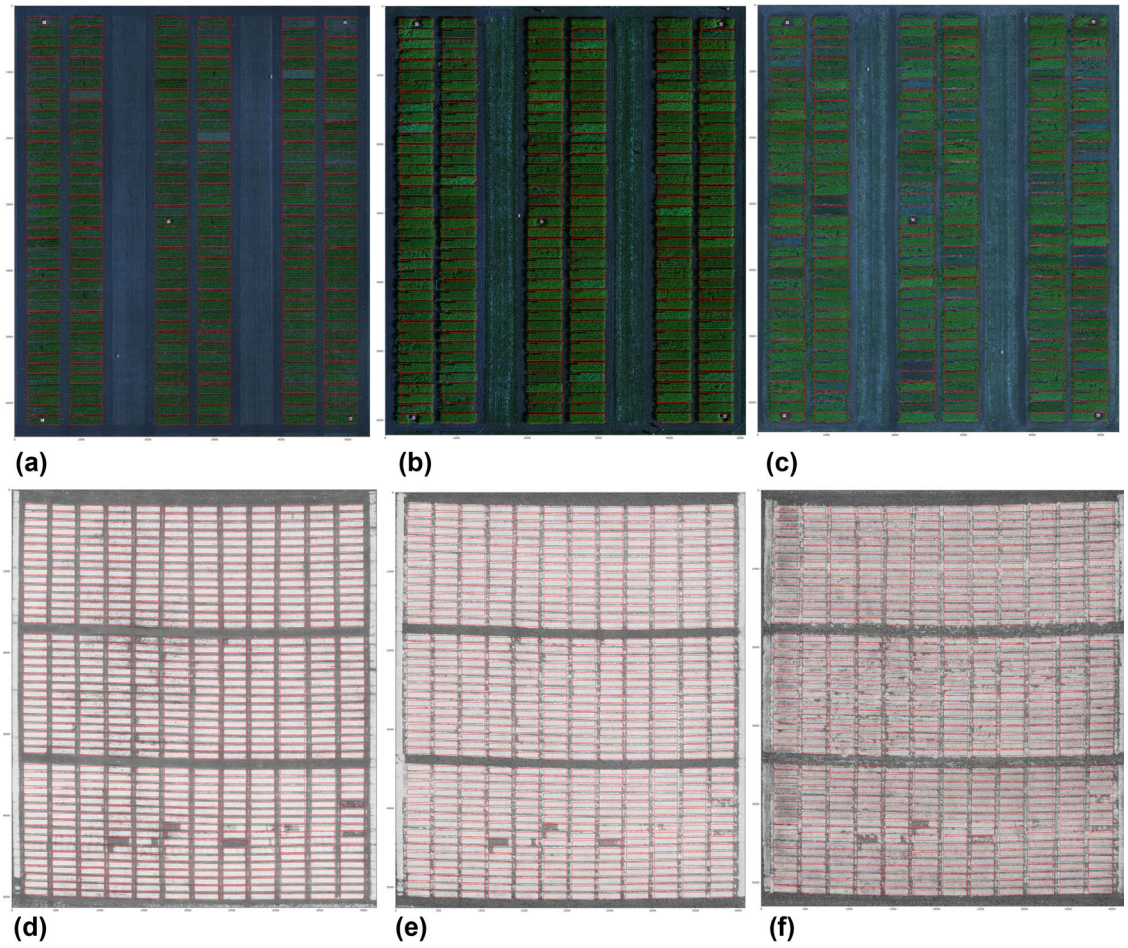

FIGURE 4 The results of the published study by (Mardanisamani et al., 2021) on the canola and wheat datasets. The results on the canola dataset (a) in early season, (b) mid-season, (c) late-season images. The results on the wheat dataset (d) in early season, (e) mid-season, and (f) late-season images

columns. Next, the number of plants per microplot is counted. Finally, the software measures canopy cover percentage and obtain vegetation indices and plant height. The software was able to analyze orthomosaic images. However, the first stage of FIELDimageR to segment the microplots was manual.

Robb et al. (2020) developed a method to segment crop microplots from aerial imagery using image processing techniques. This method was based on identifying the division between microplots to demarcate them. The authors used a combination of line detection and Hough line transform to establish the boundaries of each microplots. The proposed method used minimal input from the user and provided a high-performing technique to delineate crop microplots.

4.1.3 | Automatic methods

Automatic methods do not require manual inputs or user intervention. Parraga et al. (2018) proposed a segmentation method based on image processing techniques using UAV imagery. There are four steps, preprocessing, filtering, ROI map, and validation. This method is able to automatically segment the wheat microplots from early stages to later stages of growth. However, working for all images during the whole wheat cycle requires tuning several parameters, which results in a long time run.

Ahmed et al. (2019) developed an automatic algorithm to detect and segment lentil microplots from multispectral aerial images. They segmented vegetation/plant using NDVI and GNDVI indices. The method consisted of two phases of detection and segmentation based on Laplacian of Gaussian blob detection and a combination of unsupervised clustering and random walker methods. This method does not work correctly in late season images because neighboring microplots grow into each other and can no longer be identified as individual blobs. Also, the proposed method is unable to distinguish lentil microplots from the guard microplots. The microplots in this paper do not look rectangular because lentils grow in an unruly fashion, and that the microplots are not aligned in a grid. They are arranged in rows with fairly even spacing,

but rows are offset from each other due to the sowing process.

Mardanisamani et al. (2021) proposed a three-step image-based optimization approach to segment microplots. The authors used NDVI or ExG indices that obtained higher intensity value of vegetation than soil. This method consisted of three steps: per-block optimization, per-column optimization, and per-microplot optimization. In per-block optimization step, the position of the initial bounding box was optimized using an objective function that maximizes the sum of vegetation inside the area. In the per-column optimization step, the position of microplots' columns was optimized within their expected spacing constraints. In the last step, the authors adjusted the position of individual microplots using an objective function that simultaneously maximizes the area of the microplot's overlapping vegetation, minimizes spacing variance between microplots, and minimizes each microplot's translation relative to other microplots in the same row and column. They used RGB and NDVI orthomosaic from two wheat and canola breeding trial fields. The algorithm was able to automatically detect 99.7 and 99% of microplots for canola and wheat, respectively. Hyperparameter tuning on the whole dataset is one limitation of the proposed method that is quite time-consuming.

4.2 | Discussion and conclusion for microplot segmentation

Despite advances over previous approaches, all microplot segmentation approaches have drawbacks. The manual method does not align microplots perfectly, as the orthomosaic can be warped, or the geolocation information inaccurate. The semi-automatic methods have several drawbacks: they typically require software to create a cellular grid laid over the orthomosaic image based on the number of rows and columns. In addition, authors obtained the grid's position and attributes using external tool or by a user, and most algorithms are evaluated on one crop type and a limited number of well-spaced microplots. Furthermore, the semi-automatic methods often assume a rectangular grid and are not easily generalizable to nonrectangular arrangements of microplots. There are all drawbacks, but there will be specific situations and datasets where semi-automatic methods are viable solutions. In the automatic methods, all models have been designed and tested with orthomosaics having a relatively small number of microplots and used mid-season orthomosaic images where there is canopy closure and relatively uniform appearance of vegetation within the microplots and visible gaps in between microplots. Some proposed methods require external software to create a grid of rectangular cells manually (Khan & Miklavcic, 2019). Table 8 summarizes all studies mentioned in this section for different shapes of agricultural fields with rectangular and nonrectangular-shaped microplots. Developing an automated method to accurately extract different microplot shapes with different sizes is needed and deep-learning approaches could be used to provide a generalizable solution to address this need. Figure 4 shows the results of the published study by (Mardanisamani et al., 2021) on the canola and the wheat datasets in different growth stages.

The plant/vegetation segmentation methods for 13 microplot segmentation studies are summarized in Table 8. Nine studies were used CVI thresholding methods for vegetation segmentation. As can be seen in Table 8, CVI thresholding methods are common and important techniques to provide binary images or obtain the vegetation indices in the first step of each microplot segmentation algorithms. According to the studies, it can be concluded that segmentation of the plant/vegetation from the background is the important preprocessing step that, if done properly, will have a significant impact on improving the accuracy of microplot segmentation.

5 | DISCUSSION AND FUTURE DIRECTIONS

This paper has provided a comprehensive survey of different segmentation techniques used for vegetation and microplot segmentation. We summarized the studies on vegetation segmentation methods into three categories: VEG-based thresholding, traditional machine-learning-based, and deep-learning-based approaches. We systematically searched for papers from different online databases based on the designed research questions and finally selected 92 papers based on their relevance and quality. After reviewing and categorizing the selected papers to address the aforementioned questions, all questions are answered as follow:

Q1: What algorithms are commonly used for vegetation segmentation in the field? We reviewed various research on vegetation segmentation, aiming to identify pixels of plants or vegetation from background/soil images. Vegetation segmentation is a challenging task in agricultural image analysis. Performing this task can provide critical information about the size and shapes of regions of interest in various applications. Many researchers have proposed automated segmentation systems by applying available technologies. The early systems were built based on traditional methods such as vegetation-index-based and thresholding methods. The next wave of the methods for vegetation segmentation utilized traditional machine-learning-based approaches and became the dominant technique for many years. By the emergence of successful application of deep learning across various computer vision tasks, deep learning approaches were used for vegetation segmentation.

Q2: What algorithms are considered state-of-the-art in vegetation segmentation? Many algorithms have been used for vegetation segmentation; however, choosing the state-of-the-art algorithms in vegetation segmentation based on a literature review is challenging as these methods did not use the same dataset, making the comparison difficult. In CVI thresholding approaches, Hue, ExG, and ExGR are commonly used and recommended based on their results. Hue is robust to the variation of illumination in the field because of Hue channel image, which has the ability to represent the color of the objects in the image without any illumination effects. The ExG has advantages because it is robust to shadows. In addition, ExGR is applied to extract green regions from the background by ExG and eliminate the background noise (soil and residue) by ExR. A recent work by Lee et al. (2020) showed that the ECI outperformed Hue and ExGR. The ECI defines its function by considering pixel distributions' property, whereas all lineally formulated CVIs have empirically defined functions or were established based on data analysis.

According to the studies reviewed in the threshold-based section, it is challenging to choose a general method for finding the best threshold for different crops in different illumination conditions. The main limitation of all methods mentioned in this section is that they require some adjustments under various illumination conditions. Furthermore, since these studies used various color spaces or color indices as input images and used different datasets, some threshold methods might work for one case but not others. To overcome those challenges, finding the threshold using machine learning-based methods mentioned in the learning-based section can be applied and generalized to different illumination conditions and various stages of plant growth.

While the CVI thresholding methods are easy to implement and modify to create new CVIs, these methods are also widely used for real-time applications such as microplot segmentation. Therefore, finding a general CVI thresholding method that can be used for various crops with different illumination conditions can help improve agricultural applications' performance. The CVI thresholding method is one of the first and important preprocess steps of most agricultural applications.

Strategies using machine learning to learn more additional features generally produce better results. Extracting more features leads to obtain more information from the images. Traditional machine-learning-based approaches are often computationally efficient and applicable even in situations where we have a limited number of training samples.

Q3: How can deep learning be used to segment vegetation in images? We reviewed deep learning approaches that can be used for vegetation segmentation, including SegNet, U-Net, DeepLabV3+, and DCNN architectures. The lack of standard benchmark datasets makes comparing these architectures difficult because these architectures have been evaluated using different datasets that vary in many aspects. The study by (Morales et al., 2018) showed that DeepLabV3+ prediction accuracy compared favourably with that of the U-Net architecture while having fewer trainable parameters. The fewer parameters in DeepLabV3+ accelerate training and inference time. It also facilitates deploying DeepLabV3+ on low-cost hardware. Furthermore, the authors reported a considerable difference between the number of trainable parameters of U-Net and DeepLabV3+ due to the use of Atrous separable convolution instead of regular convolutions, significantly reducing the amount of computation.

Q4: What state-of-the-art algorithms work well in microplot segmentation in the field? To find which method obtains the best performance in microplot segmentation, we reviewed 13 papers published between 2015 and 2021. Some methods were developed only to segment rectangular-shaped microplots and some to segment nonrectangular-shaped microplots. Based on 13 studies, we recommend two methods. The first method is GRID (Chen & Zhang, 2020), which can be applied to various microplot layouts such as rhombus and zigzag patterns and grid patterns in rectangular-shaped microplots. Also, GRID can be applied without needing geolocation information. Furthermore, GRID was an effective tool to extract field microplot features. Finally, GRID produces microplot segmentation with minimal user interaction. The second method is fully automatic and proposed by Mardanisamani et al. (2019). The method automatically initialized the known field layout over the canola and wheat orthomosaic images for segmenting wheat and canola trials in roughly the right position. The algorithm relieves the processing-time bottleneck of identifying and segmenting microplots in high-throughput image-based phenotyping pipeline and simplifies the tedious pre-analysis task of identifying microplots in an orthomosaic image.

Q5: What are the future directions and research gaps? We studied the challenges and gaps in microplot segmentation. As a result, we suggest the following directions for future research.

- Deep convolutional neural networks have been successfully used in a large number of image segmentation tasks. However, to the best of our knowledge, they have not been used for microplot segmentation. We suggest deep-learning-based methods to extract and segment microplots in the field.
- Convolutional neural networks, as one of the primary parts of deep learning architectures, offer the ability to extract high-level discriminative features using a convolution kernel. A general issue with deep-learning-based method is the limited availability of open datasets in vegetation segmentation domains and limited training samples. Researchers need to develop their datasets that require many hours to produce. Therefore, new deep learning networks should be considered, such as semi-supervised learning and GANs

(Goodfellow et al., 2014). GANs are very popular in the field of deep learning methods that can be used to generate new images from scratch. To validate and compare newly developed algorithms' performance, a benchmark dataset with enough samples and corresponding ground truth annotations holds great significance. Benchmark datasets are important for researchers to work on and as a way for them to objectively measure how well their approaches doing on a particular problem. Lu and Young (2020), in their review paper, surveyed 34 public image datasets for precision agriculture. They reviewed datasets, including 15 datasets on weed control, 10 datasets on fruit detection, and 9 datasets on miscellaneous applications. Despite those datasets, a dedicated dataset on microplot segmentation is still lacking. To fill this gap, a large number of crop vision datasets with domain-specific annotation are needed. The TERRA-REF platform is a large-scale project collecting annotated sorghum and wheat microplot images and sharing them publicly. TERRA-REF can be used to characterize phenotype-to-genotype associations on a genomics scale. This benefit will develop higher-yielding cultivars of crops (LeBauer et al., 2021). Orthomosaic images in this dataset are not actual orthomosaics, and they are tiled. TERRA-REF is publicly available at https://terraref.org. ImageBreed is another online database interface that semi-automatically creates microplot images and calculates vegetation indices, currently housing millions of microplot images of alfalfa, maize, and barley field experiments across the growing season over many years (Morales et al., 2020). ImageBreed is publicly available at http://imagebreed.org. To further progress in challenging realistic agricultural conditions, we need different microplot images from various crops with different sizes and shapes. The images should be captured in various illumination conditions with annotated instances from different classes. In addition, images should be collected with different cameras and equipment and captured in a wide variety of situations. The sizes of all images should be limited by the standard input of the existing deep-learning detection network.

- In general, methods that only rely on features extracted from traditional machine learning methods often achieve lower accuracy than deep CNN models. They are also sensitive to noise. On the other hand, DCNN-based architectures often disregard research on problem-specific features. In addition, to achieve high accuracy, they require a large number of training samples. To benefit both approaches and avoid their shortcomings, designing an architecture based on features extracted from traditional machine learning-based methods and DCNN features could improve performance for small datasets. In some studies, the author focused on proposing a DCNN architecture that is not computationally demanding and makes using features extracted from machine learning-based method possible (Mardanisamani et al., 2019). Their proposed method can help to increase model accuracy, more specifically in domains where there is a limited number of training data. The fewer number of parameters in DCNN architecture accelerates training and inference time. It also facilitates deploying DCNN architecture on low-cost hardware.
- In future work, developing an algorithm that accounts for the different physical properties of various crop types and different microplot sizes is needed. This could be achieved by finding a general method based on machine learning and image processing techniques.

6 | CONCLUSION

We reviewed various research on vegetation segmentation, aiming to identify pixels of plants or vegetation from background/soil images. Vegetation segmentation is a challenging task in agricultural image analysis. Performing this task can provide critical information about the size and shapes of regions of interest in various applications. Many researchers have proposed automated segmentation systems by applying available technologies. The early systems were built based on traditional methods such as color-based and threshold-based methods. The next wave of the methods for vegetation segmentation utilized machine learning approaches and became the dominant technique for many years. Designing features has been the primary concern for developing such systems, and the complexities of this task have been considered as a significant limitation for these methods. By the emergence of successful application of deep learning across various computer vision tasks, deep learning approaches were used for vegetation segmentation.

This study showed that the selected publications use three approaches, depending on the different illumination conditions and data availability. Studies stated that vegetation-index-based thresholding approaches did not always provide the best performance for the vegetation/plant segmentation. Many machine learning algorithms have been used in different studies. The results show that no specific conclusion can be drawn as to the best algorithm, but it can be concluded that some traditional machine learning algorithms are used more than others. The most used models are the SVM, Bayesian classifier, and k-means clustering. Most of the studies used different machine-learning-based algorithms to test which algorithm had the best segmentation. Since deep learning has a large potential in other agriculture applications, we also aimed to investigate to what extent deep learning algorithms were applied for vegetation/plants segmentation. We observed that DeeplabV3+, U-Net, and SegNet architectures are the most preferred deep learning algorithms.

Plant breeding with high-throughput phenotyping can cultivate plants under extreme climatic conditions and create new

plant cultivars, resulting in increased food production. The studies for extracting and localizing microplots in the field described in this review could help any remotely sensed field trial applications, whether for weed detection/segmentation, crop rows detection, plants detection, height estimation, or yield prediction. (Mardanisamani et al., 2019; Reza et al., 2019; Lottes et al., 2020; Najafian et al., 2021). Establishing the precise location, area, and perimeter of field microplots are the first step for any of these applications. Although image-based phenotyping improves previous manual techniques, there is still substantial labor involved in identifying and segmenting microplots using manual, semi-automatic, and automatic methods.

Overall, machine vision with appropriate image processing algorithms is a very promising tool for precise real-time vegetation and microplot segmentation, providing valuable sensing information for plant phenotyping applications.

ACKNOWLEDGMENTS

This research was enabled thanks to funding from the Canada First Research Excellence Fund.

AUTHOR CONTRIBUTIONS

Sara Mardanisamani: Investigation; Methodology; Visualization; Writing – original draft; Writing – review & editing. Mark Eramian: Methodology; Project administration; Supervision; Writing – review & editing.

CONFLICT OF INTEREST

The authors declare that the research was conducted in the absence of any commercial or financial relationships that could be construed as a potential conflict of interest.

ORCID

Sara Mardanisamani https://orcid.org/0000-0001-5125-6207
Mark Eramian https://orcid.org/0000-0001-6268-5760

REFERENCES

Adams, S. M., & Friedland, C. J. (2011). A survey of unmanned aerial vehicle (UAV) usage for imagery collection in disaster research and management. In *Proceedings of the 9th International Workshop on Remote Sensing for Disaster Response, Sept. 15–16, Stanford, CA* (pp. 1–8).

Ahmed, I., Eramian, M., Ovsyannikov, I., van der Kamp, W., Nielsen, K., Duddu, H. S., Rumali, A., Shirtliffe, S., & Bett, K. (2019). Automatic detection and segmentation of lentil crop breeding plots from multi-spectral images captured by uav-mounted camera. In *2019 IEEE Winter Conference on Applications of Computer Vision (WACV), Waikoloa Village, HI* (pp. 1673–1681). IEEE.

Araus, J. L., & Cairns, J. E. (2014). Field high-throughput phenotyping: The new crop breeding frontier. *Trends in Plant Science*, *19*(1), 52–61. https://doi.org/10.1016/j.tplants.2013.09.008

Arroyo, J., Guijarro, M., & Pajares, G. (2016). An instance-based learning approach for thresholding in crop images under different outdoor conditions. *Computers and Electronics in Agriculture*, *127*, 669–679. https://doi.org/10.1016/j.compag.2016.07.018

Badrinarayanan, V., Kendall, A., & Cipolla, R. (2017). Segnet: A deep convolutional encoder-decoder architecture for image segmentation. *IEEE Transactions on Pattern Analysis and Machine Intelligence*, *39*(12), 2481–2495. https://doi.org/10.1109/TPAMI.2016.2644615

Bai, X., Cao, Z., Wang, Y., Yu, Z., Hu, Z., Zhang, X., & Li, C. (2014). Vegetation segmentation robust to illumination variations based on clustering and morphology modelling. *Biosystems Engineering*, *125*, 80–97. https://doi.org/10.1016/j.biosystemseng.2014.06.015

Bai, X., Cao, Z. - G., Wang, Y., Yu, Z., Zhang, X., & Li, C. (2013). Crop segmentation from images by morphology modeling in the cie l* a* b* color space. *Computers and Electronics in Agriculture*, *99*, 21–34. https://doi.org/10.1016/j.compag.2013.08.022

Barbosa, B., Ferraz, G., Gonçalves, L., Marin, D., Maciel, D., Ferraz, P., & Rossi, G. (2019). Rgb vegetation indices applied to grass monitoring: A qualitative analysis. *Agronomy Research*, *17*(2), 349–357.

Bendig, J., Yu, K., Aasen, H., Bolten, A., Bennertz, S., Broscheit, J., Gnyp, M. L., & Bareth, G. (2015). Combining uav-based plant height from crop surface models, visible, and near infrared vegetation indices for biomass monitoring in barley. *International Journal of Applied Earth Observation and Geoinformation*, *39*, 79–87. https://doi.org/10.1016/j.jag.2015.02.012

Bhandari, A. K., Kumar, A., & Singh, G. K. (2015). Modified artificial bee colony based computationally efficient multilevel thresholding for satellite image segmentation using kapurâ€™s, otsu and tsallis functions. *Expert Systems with Applications*, *42*(3), 1573–1601. https://doi.org/10.1016/j.eswa.2014.09.049

Biswas, H., Zhang, K., Ross, M. S., & Gann, D. (2020). Delineation of tree patches in a mangrove-marsh transition zone by watershed segmentation of aerial photographs. *Remote Sensing*, *12*(13), 2086. https://doi.org/10.3390/rs12132086

Breiman, L., Friedman, J., Olshen, R., & Stone, C. (1984). *Classification and regression trees*. Wadsworth International Group.

Burgos-Artizzu, X. P., Ribeiro, A., Guijarro, M., & Pajares, G. (2011). Real-time image processing for crop/weed discrimination in maize fields. *Computers and Electronics in Agriculture*, *75*(2), 337–346. https://doi.org/10.1016/j.compag.2010.12.011

Campos, Y., Rodner, E., Denzler, J., Sossa, H., & Pajares, G. (2016). Vegetation segmentation in cornfield images using bag of words. In J. Blanc-Talon, C. Distante, W. Philips, D. Popescu, & P. Scheunders (Eds.), *International Conference on Advanced Concepts for Intelligent Vision Systems* (pp. 193–204). Springer.

Chang, C. Y., Zhou, R., Kira, O., Marri, S., Skovira, J., Gu, L., & Sun, Y. (2020). An unmanned aerial system (uas) for concurrent measurements of solar-induced chlorophyll fluorescence and hyperspectral reflectance toward improving crop monitoring. *Agricultural and Forest Meteorology*, *294*, 108145. https://doi.org/10.1016/j.agrformet.2020.108145

Chawade, A., van Ham, J., Blomquist, H., Bagge, O., Alexandersson, E., & Ortiz, R. (2019). High-throughput field-phenotyping tools for plant breeding and precision agriculture. *Agronomy*, *9*(5), 258. https://doi.org/10.3390/agronomy9050258

Chebrolu, N., Lottes, P., Schaefer, A., Winterhalter, W., Burgard, W., & Stachniss, C. (2017). Agricultural robot dataset for plant classification, localization and mapping on sugar beet fields. *The International*

Journal of Robotics Research, *36*(10), 1045–1052. https://doi.org/10.1177/0278364917720510

Chen, C. J., & Zhang, Z. (2020). Grid: A python package for field plot phenotyping using aerial images. *Remote Sensing*, *12*(11), 1697. https://doi.org/10.3390/rs12111697

Chen, L. - C., Papandreou, G., Kokkinos, I., Murphy, K., & Yuille, A. L. (2017). Deeplab: Semantic image segmentation with deep convolutional nets, atrous convolution, and fully connected crfs. *IEEE Transactions on Pattern Analysis and Machine Intelligence*, *40*(4), 834–848. https://doi.org/10.1109/TPAMI.2017.2699184

Chen, L. - C., Papandreou, G., Schroff, F., & Adam, H. (2017). Rethinking atrous convolution for semantic image segmentation. arXiv preprint arXiv:1706.05587.

Cheng, H. - D., Jiang, X. H., Sun, Y., & Wang, J. (2001). Color image segmentation: Advances and prospects. *Pattern Recognition*, *34*(12), 2259–2281. https://doi.org/10.1016/S0031-3203(00)00149-7

Coy, A., Rankine, D., Taylor, M., Nielsen, D. C., & Cohen, J. (2016). Increasing the accuracy and automation of fractional vegetation cover estimation from digital photographs. *Remote Sensing*, *8*(7), 474. https://doi.org/10.3390/rs8070474

Crnic, J. (2011). *Introduction to modern information retrieval*. Library Management.

Duan, T., Zheng, B., Guo, W., Ninomiya, S., Guo, Y., & Chapman, S. C. (2017). Comparison of ground cover estimates from experiment plots in cotton, sorghum and sugarcane based on images and orthomosaics captured by UAV. *Functional Plant Biology*, *44*(1), 169–183. https://doi.org/10.1071/FP16123

Fuentes-Pacheco, J., Torres-Olivares, J., Roman-Rangel, E., Cervantes, S., Juarez-Lopez, P., Hermosillo-Valadez, J., & Rendón-Mancha, J. M. (2019). Fig plant segmentation from aerial images using a deep convolutional encoder-decoder network. *Remote Sensing*, *11*(10), 1157. https://doi.org/10.3390/rs11101157

Fuentes-Penailillo, F., Ortega-Farias, S., Rivera, M., Bardeen, M., & Moreno, M. (2018). Using clustering algorithms to segment uav-based rgb images. In *2018 IEEE International Conference on Automation/XXIII Congress of the Chilean Association of Automatic Control (ICA-ACCA)* (pp. 1–5) IEEE.

Gitelson, A. A., Kaufman, Y. J., Stark, R., & Rundquist, D. (2002). Novel algorithms for remote estimation of vegetation fraction. *Remote Sensing of Environment*, *80*(1), 76–87. https://doi.org/10.1016/S0034-4257(01)00289-9

Golzarian, M. R., & Frick, R. A. (2011). Classification of images of wheat, ryegrass and brome grass species at early growth stages using principal component analysis. *Plant Methods*, *7*(1), 28. https://doi.org/10.1186/1746-4811-7-28

Golzarian, M. R., Lee, M. - K., & Desbiolles, J. (2012). Evaluation of color indices for improved segmentation of plant images. *Transactions of the ASABE*, *55*(1), 261–273. https://doi.org/10.13031/2013.41236

Goodfellow, I. J., Pouget-Abadie, J., Mirza, M., Xu, B., Warde-Farley, D., Ozair, S., Courville, A., & Bengio, Y. (2014). Generative adversarial networks. *arXiv*.

Guerrero, J. M., Pajares, G., Montalvo, M., Romeo, J., & Guijarro, M. (2012). Support vector machines for crop/weeds identification in maize fields. *Expert Systems with Applications*, *39*(12), 11149–11155. https://doi.org/10.1016/j.eswa.2012.03.040

Guijarro, M., Pajares, G., Riomoros, I., Herrera, P., Burgos-Artizzu, X., & Ribeiro, A. (2011). Automatic segmentation of relevant textures in agricultural images. *Computers and Electronics in Agriculture*, *75*(1), 75–83. https://doi.org/10.1016/j.compag.2010.09.013

Guijarro, M., Riomoros, I., Pajares, G., & Zitinski, P. (2015). Discrete wavelets transform for improving greenness image segmentation in agricultural images. *Computers and Electronics in Agriculture*, *118*, 396–407. https://doi.org/10.1016/j.compag.2015.09.011

Guo, W., Rage, U. K., & Ninomiya, S. (2013). Illumination invariant segmentation of vegetation for time series wheat images based on decision tree model. *Computers and Electronics in Agriculture*, *96*, 58–66. https://doi.org/10.1016/j.compag.2013.04.010

Guo, W., Zheng, B., Potgieter, A. B., Diot, J., Watanabe, K., Noshita, K., Jordan, D., Wang, X., Watson, J., & Ninomiya, S. (2018). Aerial imagery analysis: Quantifying appearance and number of sorghum heads for applications in breeding and agronomy. *Frontiers in Plant Science*, *9*, 1544. https://doi.org/10.3389/fpls.2018.01544

Haghighattalab, A., Pérez, L. G., Mondal, S., Singh, D., Schinstock, D., Rutkoski, J., Ortiz-Monasterio, I., Singh, R. P., Goodin, D., & Poland, J. (2016). Application of unmanned aerial systems for high throughput phenotyping of large wheat breeding nurseries. *Plant Methods*, *12*(1), 35. https://doi.org/10.1186/s13007-016-0134-6

Hague, T., Tillett, N., & Wheeler, H. (2006). Automated crop and weed monitoring in widely spaced cereals. *Precision Agriculture*, *7*(1), 21–32. https://doi.org/10.1007/s11119-005-6787-1

Hamuda, E., Glavin, M., & Jones, E. (2016). A survey of image processing techniques for plant extraction and segmentation in the field. *Computers and Electronics in Agriculture*, *125*, 184–199. https://doi.org/10.1016/j.compag.2016.04.024

Hassanein, M., Lari, Z., & El-Sheimy, N. (2018). A new vegetation segmentation approach for cropped fields based on threshold detection from hue histograms. *Sensors*, *18*(4), 1253. https://doi.org/10.3390/s18041253

Hearst, A. A., & Cherkauer, K. A. (2015). Extraction of small spatial plots from geo-registered UAS imagery of crop fields. *Environmental Practice*, *17*(3), 178–187. https://doi.org/10.1017/S1466046615000162

Ho, T. K. (1998). The random subspace method for constructing decision forests. *IEEE Transactions on Pattern Analysis and Machine Intelligence*, *20*(8), 832–844.

Hunt, E. R., Cavigelli, M., Daughtry, C. S., Mcmurtrey, J. E., & Walthall, C. L. (2005). Evaluation of digital photography from model aircraft for remote sensing of crop biomass and nitrogen status. *Precision Agriculture*, *6*(4), 359–378. https://doi.org/10.1007/s11119-005-2324-5

Hunt Jr, E. R., Daughtry, C., Eitel, J. U., & Long, D. S. (2011). Remote sensing leaf chlorophyll content using a visible band index. *Agronomy Journal*, *103*(4), 1090–1099. https://doi.org/10.2134/agronj2010.0395

Hunt Jr, E. R., Doraiswamy, P. C., McMurtrey, J. E., Daughtry, C. S., Perry, E. M., & Akhmedov, B. (2013). A visible band index for remote sensing leaf chlorophyll content at the canopy scale. *International Journal of Applied Earth Observation and Geoinformation*, *21*, 103–112. https://doi.org/10.1016/j.jag.2012.07.020

Jeon, H. Y., Tian, L. F., & Zhu, H. (2011). Robust crop and weed segmentation under uncontrolled outdoor illumination. *Sensors*, *11*(6), 6270–6283. https://doi.org/10.3390/s110606270

Kamilaris, A., & Prenafeta-Boldú, F. X. (2018). Deep learning in agriculture: A survey. *Computers and Electronics in Agriculture*, *147*, 70–90. https://doi.org/10.1016/j.compag.2018.02.016

Kataoka, T., Kaneko, T., Okamoto, H., & Hata, S. (2003). Crop growth estimation system using machine vision. In *Proceedings 2003 IEEE/ASME International Conference on Advanced Intelligent Mechatronics (AIM 2003)* (Vol. 2, pp. b1079–b1083). IEEE.

Keller, K., Kirchgessner, N., Khanna, R., Siegwart, R., Walter, A., & Aasen, H. (2018). Soybean leaf coverage estimation with machine learning and thresholding algorithms for field phenotyping. In *Proceedings of the British Machine Vision Conference, Newcastle, UK* (pp. 3–6). BMVA Press.

Khan, Z., & Miklavcic, S. J. (2019). An automatic field plot extraction method from aerial orthomosaic images. *Frontiers in Plant Science*, *10*, 683. https://doi.org/10.3389/fpls.2019.00683

Kirk, K., Andersen, H. J., Thomsen, A. G., Jørgensen, J. R., & Jørgensen, R. N. (2009). Estimation of leaf area index in cereal crops using red–green images. *Biosystems Engineering*, *104*(3), 308–317. https://doi.org/10.1016/j.biosystemseng.2009.07.001

Kumar, D. A., & Prema, P. (2013). A review on crop and weed segmentation based on digital images. In P. P. Swamy & D. S. Guru (Eds.), *Multimedia processing, communication and computing applications* (pp. 279–291). Springer.

LeBauer, D., Burnette, M., Fahlgren, N., Kooper, R., McHenry, K., & Stylianou, A. (2021). What does terra-ref's high resolution, multi sensor plant sensing public domain data offer the computer vision community? In *Proceedings of the IEEE/CVF International Conference on Computer Vision (ICCV) Workshops* (pp. 1409–1415).

Lee, M. K., Golzarian, M. R., & Kim, I. (2020). A new color index for vegetation segmentation and classification. *Precision Agriculture*, *22*(1), 179–204.

Li, L., Mu, X., Macfarlane, C., Song, W., Chen, J., Yan, K., & Yan, G. (2018). A half-gaussian fitting method for estimating fractional vegetation cover of corn crops using unmanned aerial vehicle images. *Agricultural and Forest Meteorology*, *262*, 379–390. https://doi.org/10.1016/j.agrformet.2018.07.028

Liu, Y., Mu, X., Wang, H., & Yan, G. (2012). A novel method for extracting green fractional vegetation cover from digital images. *Journal of Vegetation Science*, *23*(3), 406–418. https://doi.org/10.1111/j.1654-1103.2011.01373.x

Lottes, P., Behley, J., Chebrolu, N., Milioto, A., & Stachniss, C. (2020). Robust joint stem detection and crop-weed classification using image sequences for plant-specific treatment in precision farming. *Journal of Field Robotics*, *37*(1), 20–34. https://doi.org/10.1002/rob.21901

Louhaichi, M., Borman, M. M., & Johnson, D. E. (2001). Spatially located platform and aerial photography for documentation of grazing impacts on wheat. *Geocarto International*, *16*(1), 65–70. https://doi.org/10.1080/10106040108542184

Lu, H., Cao, Z., Xiao, Y., Li, Y., & Zhu, Y. (2016). Region-based colour modelling for joint crop and maize tassel segmentation. *Biosystems Engineering*, *147*, 139–150. https://doi.org/10.1016/j.biosystemseng.2016.04.007

Lu, Y., & Young, S. (2020). A survey of public datasets for computer vision tasks in precision agriculture. *Computers and Electronics in Agriculture*, *178*, 105760. https://doi.org/10.1016/j.compag.2020.105760

Mardanisamani, S., Ayalew, T. W., Badhon, M. A., Khan, N. A., Hasnat, G., Duddu, H., Shirtliffe, S., Vail, S., Stavness, I., & Eramian, M. (2021). Automatic microplot localization using UAV images and a hierarchical image-based optimization method. *Plant Phenomics*, *2021*, 9764514.

Mardanisamani, S., Maleki, F., Hosseinzadeh Kassani, S., Rajapaksa, S., Duddu, H., Wang, M., Shirtliffe, S., Ryu, S., Josuttes, A., Zhang, T., Vail, S., Pozniak, C., Parkin, I., Stavness, I., & Eramian, M. (2019). Crop lodging prediction from UAV-acquired images of wheat and canola using a DCNN augmented with handcrafted texture features. In *Proceedings of the IEEE Conference on Computer Vision and Pattern Recognition Workshops* (pp. 2657–2664). IEEE.

Maresma, Á., Ariza, M., Martnez, E., Lloveras, J., & Martnez-Casasnovas, J. A. (2016). Analysis of vegetation indices to determine nitrogen application and yield prediction in maize (*Zea Mays* L.) from a standard UAV service. *Remote Sensing*, *8*(12), 973. https://doi.org/10.3390/rs8120973

Matias, F. I., Caraza-Harter, M. V., & Endelman, J. B. (2020). FieldimageR: An R package to analyze orthomosaic images from agricultural field trials. *The Plant Phenome Journal*, https://doi.org/10.1002/ppj2.20005

Meyer, G. E., & Neto, J. C. (2008). Verification of color vegetation indices for automated crop imaging applications. *Computers and Electronics in Agriculture*, *63*(2), 282–293. https://doi.org/10.1016/j.compag.2008.03.009

Meyer, G. E., Neto, J. C., Jones, D. D., & Hindman, T. W. (2004). Intensified fuzzy clusters for classifying plant, soil, and residue regions of interest from color images. *Computers and Electronics in Agriculture*, *42*(3), 161–180. https://doi.org/10.1016/j.compag.2003.08.002

Milioto, A., Lottes, P., & Stachniss, C. (2018). Real-time semantic segmentation of crop and weed for precision agriculture robots leveraging background knowledge in CNNs. In *2018 IEEE International Conference on Robotics and Automation (ICRA)* (pp. 2229–2235). IEEE.

Montalvo, M., Guijarro, M., Guerrero, J. M., & Ribeiro, Á. (2016). Identification of plant textures in agricultural images by principal component analysis. In *International Conference on Hybrid Artificial Intelligence Systems* (pp. 391–401). Springer.

Montalvo, M., Guijarro, M., & Ribeiro, A. (2018). A novel threshold to identify plant textures in agricultural images by otsu and principal component analysis. *Journal of Intelligent & Fuzzy Systems*, *34*(6), 4103–4111.

Moorthy, S., Boigelot, B., & Mercatoris, B. (2015). Effective segmentation of green vegetation for resource-constrained real-time applications. In J. V. Stafford, *Precision agriculture* (pp. 93–98). Wageningen Academic Publishers.

Morales, G., Kemper, G., Sevillano, G., Arteaga, D., Ortega, I., & Telles, J. (2018). Automatic segmentation of mauritia flexuosa in unmanned aerial vehicle (UAV) imagery using deep learning. *Forests*, *9*(12), 736. https://doi.org/10.3390/f9120736

Morales, N., Kaczmar, N. S., Santantonio, N., Gore, M. A., Mueller, L. A., & Robbins, K. R. (2020). Imagebreed: Open-access plant breeding web–database for image-based phenotyping. *The Plant Phenome Journal*, *3*(1), e20004. https://doi.org/10.1002/ppj2.20004

Najafian, K., Ghanbari, A., Stavness, I., Jin, L., Shirdel, G. H., & Maleki, F. (2021). A semi-self-supervised learning approach for wheat head detection using extremely small number of labeled samples. In *Proceedings of the IEEE/CVF International Conference on Computer Vision (ICCV) Workshops* (pp. 1342–1351). IEEE.

Neto, J. C. (2004). *A combined statistical-soft computing approach for classification and mapping weed species in minimum-tillage systems*. The University of Nebraska-Lincoln.

Netto, A., Martins, R. N., de Souza, G., Araújo, G. d. M., de Almeida, S., & Capelini, V. A. (2018). Segmentation of rgb images using different vegetation indices and thresholding methods. *Nativa:*

Pesquisas Agrárias e Ambientais, *6*(4), 389–394. https://doi.org/10.31413/nativa.v6i4.5405

Otsu, N. (1979). A threshold selection method from gray-level histograms. *IEEE Transactions on Systems, Man, and Cybernetics*, *9*(1), 62–66. https://doi.org/10.1109/TSMC.1979.4310076

Ozyavuz, M., Bilgili, B., & Salici, A. (2015). Determination of vegetation changes with ndvi method. *Journal of Environmental Protection and Ecology*, *16*(1), 264–273.

Parraga, A., Doering, D., Atkinson, J. G., Bertani, T., de Oliveira Andrades Filho, C., de Souza, M. R. Q., Ruschel, R., & Susin, A. A. (2018). Wheat plots segmentation for experimental agricultural field from visible and multispectral UAV imaging. In *Proceedings of SAI Intelligent Systems Conference* (pp. 388–399). Springer.

Pinguet, B. (2021). The role of drone technology in sustainable agriculture. Precision Ag.

Recio, J., Hermosilla, T., Ruiz, L., & Palomar, J. (2013). Automated extraction of tree and plot-based parameters in citrus orchards from aerial images. *Computers and Electronics in Agriculture*, *90*, 24–34. https://doi.org/10.1016/j.compag.2012.10.005

Reza, M. N., Na, I. S., Baek, S. W., & Lee, K. - H. (2019). Rice yield estimation based on K-means clustering with graph-cut segmentation using low-altitude UAV images. *Biosystems Engineering*, *177*, 109–121. https://doi.org/10.1016/j.biosystemseng.2018.09.014

Ribera Prat, J. (2019). *Image-based plant phenotyping using machine learning* [PhD thesis]. Purdue University Graduate School.

Rico-Fernández, M., Rios-Cabrera, R., Castelán, M., Guerrero-Reyes, H. - I., & Juarez-Maldonado, A. (2019). A contextualized approach for segmentation of foliage in different crop species. *Computers and Electronics in Agriculture*, *156*, 378–386. https://doi.org/10.1016/j.compag.2018.11.033

Robb, C., Hardy, A., Doonan, J. H., & Brook, J. (2020). Semi-automated field plot segmentation from uas imagery for experimental agriculture. *Frontiers in Plant Science*, 11.

Ronneberger, O., Fischer, P., & Brox, T. (2015). U-net: Convolutional networks for biomedical image segmentation. In *International Conference on Medical image computing and computer-assisted intervention* (pp. 234–241). Springer.

Rouse Jr, J., Haas, R., Schell, J., & Deering, D. (1974). *Monitoring vegetation systems in the Great Plains with ERTS* (Vol. 351). NASA.

Ruiz-Ruiz, G., Gómez-Gil, J., & Navas-Gracia, L. (2009). Testing different color spaces based on hue for the environmentally adaptive segmentation algorithm (EASA). *Computers and Electronics in Agriculture*, *68*(1), 88–96. https://doi.org/10.1016/j.compag.2009.04.009

Sadeghi-Tehran, P., Virlet, N., Sabermanesh, K., & Hawkesford, M. J. (2017). Multi-feature machine learning model for automatic segmentation of green fractional vegetation cover for high-throughput field phenotyping. *Plant Methods*, *13*(1), 103. https://doi.org/10.1186/s13007-017-0253-8

Saha, D., Hanson, A., & Shin, S. Y. (2016). Development of enhanced weed detection system with adaptive thresholding and support vector machine. In *Proceedings of the International Conference on Research in Adaptive and Convergent Systems* (pp. 85–88). Association for Computing Machinery.

Sishodia, R. P., Ray, R. L., & Singh, S. K. (2020). Applications of remote sensing in precision agriculture: A review. *Remote Sensing*, *12*(19), 3136. https://doi.org/10.3390/rs12193136

Tausen, M., Clausen, M., Moeskjær, S., Shihavuddin, A., Dahl, A. B., Janss, L., & Andersen, S. U. (2020). Greenotyper: Image-based plant phenotyping using distributed computing and deep learning. *Frontiers in Plant Science*, *11*, 1181. https://doi.org/10.3389/fpls.2020.01181

Tian, L. F., & Slaughter, D. C. (1998). Environmentally adaptive segmentation algorithm for outdoor image segmentation. *Computers and Electronics in Agriculture*, *21*(3), 153–168. https://doi.org/10.1016/S0168-1699(98)00037-4

Torres-Sánchez, J., López-Granados, F., De Castro, A. I., & Peña-Barragán, J. M. (2013). Configuration and specifications of an unmanned aerial vehicle (UAV) for early site specific weed management. *Plos One*, *8*(3), e58210. https://doi.org/10.1371/journal.pone.0058210

Torres-Sánchez, J., López-Granados, F., & Peña, J. M. (2015). An automatic object-based method for optimal thresholding in uav images: Application for vegetation detection in herbaceous crops. *Computers and Electronics in Agriculture*, *114*, 43–52. https://doi.org/10.1016/j.compag.2015.03.019

Torres-Sánchez, J., Pena, J. M., de Castro, A. I., & López-Granados, F. (2014). Multi-temporal mapping of the vegetation fraction in early-season wheat fields using images from uav. *Computers and Electronics in Agriculture*, *103*, 104–113. https://doi.org/10.1016/j.compag.2014.02.009

Tresch, L., Mu, Y., Itoh, A., Kaga, A., Taguchi, K., Hirafuji, M., Ninomiya, S., & Guo, W. (2019). Easy MPE: Extraction of quality microplot images for UAV-based high-throughput field phenotyping. *Plant Phenomics*, *2019*, 2591849. https://doi.org/10.34133/2019/2591849

Wang, A., Zhang, W., & Wei, X. (2019). A review on weed detection using ground-based machine vision and image processing techniques. *Computers and Electronics in Agriculture*, *158*, 226–240. https://doi.org/10.1016/j.compag.2019.02.005

Woebbecke, D. M., Meyer, G. E., Von Bargen, K., & Mortensen, D. A. (1993). Plant species identification, size, and enumeration using machine vision techniques on near-binary images. In *Optics in agriculture and forestry* (Vol. 1836, pp. 208–219). International Society for Optics and Photonics.

Woebbecke, D. M., Meyer, G. E., Von Bargen, K., & Mortensen, D. A. (1995). Color indices for weed identification under various soil, residue, and lighting conditions. *Transactions of the ASAE*, *38*(1), 259–269. https://doi.org/10.13031/2013.27838

Xu, M., Liu, M., Liu, F., Zheng, N., Tang, S., Zhou, J., Ma, Q., & Wu, L. (2021). A safe, high fertilizer-efficiency and economical approach based on a low-volume spraying uav loaded with chelated-zinc fertilizer to produce zinc-biofortified rice grains. *Journal of Cleaner Production*, *323*, 129188. https://doi.org/10.1016/j.jclepro.2021.129188

Xu, R., Li, C., & Paterson, A. H. (2019). Multispectral imaging and unmanned aerial systems for cotton plant phenotyping. *Plos One*, *14*(2), e0205083. https://doi.org/10.1371/journal.pone.0205083

Yang, C., Baireddy, S., Cai, E., Crawford, M., & Delp, E. J. (2021). Field-based plot extraction using uav rgb images. In *Proceedings of the IEEE/CVF International Conference on Computer Vision* (ICCV) Workshops (pp. 1390–1398).

Yang, W., Zhao, X., Wang, S., Chen, L., Chen, X., & Lu, S. (2015). A new approach for greenness identification from maize images. In *International Conference on Intelligent Computing* (pp. 339–347). Springer.

Ye, M., Cao, Z., Yu, Z., & Bai, X. (2015). Crop feature extraction from images with probabilistic superpixel markov random field. *Computers and Electronics in Agriculture*, *114*, 247–260. https://doi.org/10.1016/j.compag.2015.04.010

Yu, Z., Cao, Z., Wu, X., Bai, X., Qin, Y., Zhuo, W., Xiao, Y., Zhang, X., & Xue, H. (2013). Automatic image-based detection technology for two critical growth stages of maize: Emergence and three-leaf stage. *Agricultural and Forest Meteorology*, *174*, 65–84. https://doi.org/10.1016/j.agrformet.2013.02.011

Zheng, L., Shi, D., & Zhang, J. (2010). Segmentation of green vegetation of crop canopy images based on mean shift and Fisher linear discriminant. *Pattern Recognition Letters*, *31*(9), 920–925. https://doi.org/10.1016/j.patrec.2010.01.016

Zheng, L., Zhang, J., & Wang, Q. (2009). Mean-shift-based color segmentation of images containing green vegetation. *Computers and Electronics in Agriculture*, *65*(1), 93–98. https://doi.org/10.1016/j.compag.2008.08.002

Zhuang, S., Wang, P., & Jiang, B. (2018). Segmentation of green vegetation in the field using deep neural networks. In *13th World Congress on Intelligent Control and Automation (WCICA)* (pp. 509–514). IEEE.

Zhuang, S., Wang, P., & Jiang, B. (2020). Vegetation extraction in the field using multi-level features. *Biosystems Engineering*, *197*, 352–366. https://doi.org/10.1016/j.biosystemseng.2020.07.013

How to cite this article: Mardanisamani, S., & Eramian, M. (2022). Segmentation of vegetation and microplots in aerial agriculture images: A survey. *The Plant Phenome Journal*, *5,* e20042. https://doi.org/10.1002/ppj2.20042